R/D 5882-PH-01-2

②

AD-A199 178

STUDY ON IRON DISILICIDE

THERMOELECTRIC GENERATOR

by

John G. STOCKHOLM
Hubert SCHERRER
Philippe SCHLICKLIN

May 1988

United States Army

EUROPEAN RESEARCH OFFICE OF THE U.S. ARMY

London   England

CONTRACT NUMBER = DAJA45-87-C-0057

TNEE

DTIC
SELECTED
SEP 2 0 1988
E

88 9

REPORT DOCUMENTATION PAGE	Form Approved OMB No. 0704-0188

a. REPORT SECURITY CLASSIFICATION	1b. RESTRICTIVE MARKINGS

2a. SECURITY CLASSIFICATION AUTHORITY	3 DISTRIBUTION / AVAILABILITY OF REPORT
b. DECLASSIFICATION / DOWNGRADING SCHEDULE	

4. PERFORMING ORGANIZATION REPORT NUMBER(S)	5. MONITORING ORGANIZATION REPORT NUMBER(S)
N° 2	

6a. NAME OF PERFORMING ORGANIZATION	6b. OFFICE SYMBOL (If applicable)	7a. NAME OF MONITORING ORGANIZATION
T N E E		

6c. ADDRESS (City, State, and ZIP Code)	7b. ADDRESS (City, State, and ZIP Code)
250, route de l'Empereur 92508 RUEIL MALMAISON — FRANCE	

8a. NAME OF FUNDING / SPONSORING ORGANIZATION European Research Office of U.S. Army	8b. OFFICE SYMBOL (If applicable)	9. PROCUREMENT INSTRUMENT IDENTIFICATION NUMBER

8c. ADDRESS (City, State, and ZIP Code)	10. SOURCE OF FUNDING NUMBERS			
223-231 Old Marylebone Road LONDON N W 1 - 5 T H	PROGRAM ELEMENT NO.	PROJECT NO. R-D 5882 PH 01	TASK NO.	WORK UNIT ACCESSION NO

11. TITLE (Include Security Classification)

STUDY ON IRON DISILICIDE THERMOELECTRIC GENERATOR

12. PERSONAL AUTHOR(S)
SCHERRER Hubert, SCHLICKLIN Philippe, STOCKHOLM John

3a. TYPE OF REPORT Periodic	13b. TIME COVERED FROM Oct 87 TO Feb 89	14. DATE OF REPORT (Year, Month, Day) 1988 June 15	15. PAGE COUNT 91

6. SUPPLEMENTARY NOTATION

17. COSATI CODES			18 SUBJECT TERMS (Continue on reverse if necessary and identify by block number)
FIELD	GROUP	SUB-GROUP	Thermoelectricity Iron disilicide

9. ABSTRACT (Continue on reverse if necessary and identify by block number)

A theorical study is done on the thermoelectric material iron disilicide. The N type is doped with Cobalt, the P type can either be doped Al or Mn.

A small prototype is built enabling heat flux measurements. The efficiencies were measured for the KOMATSU couples which have Al doped P typed logs. The Unit produced with 18 couples 0.75 watts. The efficiency of a couple alone (ration of electrical power by thermal power through the couple) is around 1 %.

0. DISTRIBUTION / AVAILABILITY OF ABSTRACT ☒ UNCLASSIFIED/UNLIMITED ☐ SAME AS RPT ☐ DTIC USERS	21. ABSTRACT SECURITY CLASSIFICATION
2a. NAME OF RESPONSIBLE INDIVIDUAL John G. STOCKHOLM	22b TELEPHONE (Include Area Code) 33.1.47.52.58.29. 22c. OFFICE SYMBOL

DD Form 1473, JUN 86   *Previous editions are obsolete.*

1

STUDY ON IRON DISILICIDE

THERMOELECTRIC GENERATOR

Principal Investigator :

John G. STOCKHOLM

United States Army

EUROPEAN RESEARCH OFFICE OF THE U.S. ARMY

London England

CONTRACT NUMBER = DAJA45-87-C-0057

2nd Periodic Report - June 1988

TNEE

October 1987 - February 1988

Accession For	
NTIS GRA&I	☒
DTIC TAB	☐
Unannounced	☐
Justification	
By	
Distribution/	
Availability Codes	
Dist	Avail and/or Special
A-1	

IRON DISILICIDE THERMOELECTRIC GENERATOR

FEASIBILITY STUDY

This study has two parts, a theoretical analysis of the material Iron Disilicide and an experimental work based on a thermal flux prototype.

PART ONE   Dr. Hubert SCHERRER

The theoretical aspect covers several topics :

- massive Iron Disilicide
  This is the only manufacturing process which is used industrially today and to our knowledge only in Japan. The properties of this material are presented and the material $FeSi_2$ is examined in detail.

- a new amorphous material seems interesting, one of its applications would be in thin film technology, if its stability is proven for the operating conditions.

PART TWO   Dr. Philippe SCHLICKLIN

Iron Disilicide couples are used in Japan to generate very small electrical powers for the controls of gas heaters. The object of this study is to measure the efficiency of these couples ; by efficiency we mean the ratio of the generated electrical power to the heat that goes through the couple.

A small prototype designed to be able to estimate the heat going through the couples was built and tested.

Comparisons with the manufacturer's data are made and also the results were compared with those of a material manufactured by the University of Karlsruhe (West Germany).

PART 1

THEORETICAL ANALYSIS OF IRON DISILICIDE

A REVIEW OF SEMICONDUCTING AND

THERMOELECTRIC PROPERTIES OF IRON DISILICIDE

H. SCHERRER

Lab. Physique du Solide. UA 155

Ecole des Mines

Parc de Saurupt

54042 NANCY CEDEX, FRANCE

INTRODUCTION

Using the accessible data bases, we are collecting some international publications (USA, Japan, Soviet Union, France, Germany ...). We present the phase diagram of the system Fe-Si. The preparation of the β-FeSi$_2$ semiconducting phasis is described. From the bibliography we report and analyse the thermal properties (thermoelectric power, electrical and thermal conductivity) for the intrinsic and doped (Co, Mn, Al) material. We exibit the figure of merit of n and p-type FeSi$_2$ as a function of the temperature for optimized doping. Then we give some conclusions about the advantages or disadvantages of this material. We conclude on a review about new amorphous material, thinking that their thermoelectric properties must be checked after prolonged thermal heating.

5

I-1 PHASE DIAGRAM OF THE BINARY SYSTEM Fe-Si

According to the phase diagram of the binary
system [1-5] the compound $FeSi_2$ exists in a metallic high tem-
perature phase (α-$FeSi_2$) and a semiconducting low temperature
phase (β-$FeSi_2$). (Fig. I).

The transition temperature is 1228 K. The metallic
phase is eutectic alloy consisting of FeSi and $Fe_{1-\alpha}Si_2$ and
the semiconducting one which is stoichiometric, $FeSi_2$. The
metallic phase which is unstable at high temperatures becomes
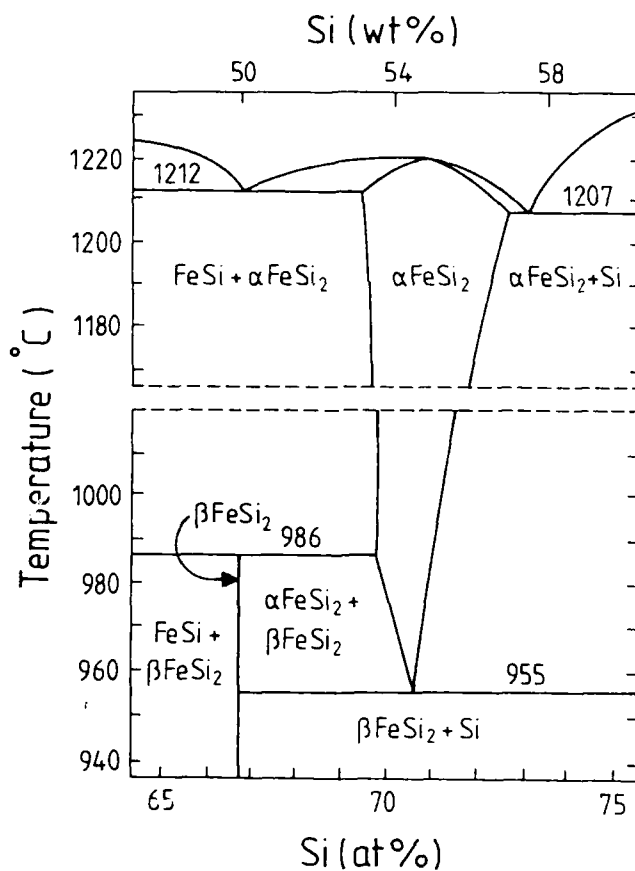stable $FeSi_2$ with the semiconducting property below 1259 K.

Fig. I Phase diagram of the binary system Fe-Si.

I-2 $\alpha \rightarrow \beta$ PHASE TRANSFORMATION

$FeSi_2$ is of interest because of thermoelectrical properties of the β phase and because the electrical properties show a metal-nonmetal transition [6-11].

In $FeSi_2$ the transition has been treated as a generalized Jahn-Teller distortion [12]. In this picture a distortion of the lattice is coupled to a shift of the one electron energy levels, resulting in an energy gap, while the total energy of the occupied electronic states is lowered. In our opinion the determination of the β-$FeSi_2$ structure [13] invalidates this description, because besides a distortion of the Si sublattice it is necessary to assume a migration of the Fe atoms through this sublattice [14] and a formation of Fe vacancies in going from the β to the α phase. α-$FeSi_2$ has a simple structure. In figure II the unit cell is given, which contains only three atoms. The Fe atoms are almost cubically surrounded by eight Si atoms at a distance of 2.35 Å and by four Fe atoms in the XOY plane at 2.68 Å. However, the situation is complicated by the fact that the Fe sublattice contains 13-23 % vacancies [15]. This means we have distribution of Fe surroundings instead of a crystallographic equivalence of all the Fe atoms.

Though the β-$FeSi_2$ structure is not complicated by deviations from stoichiometry it contains 48 atoms per unit cell and has a very low symmetry. A detailed determination is given by Dusausoy et al, its spatial group is Cmca with the parameters a = 9,863 Å b = 7,791 Å c = 7,833 Å [13]. Here, as in

the α phase, we have a sublattice of deformed Si cubes, half of which contain an Fe atom. Every second cube is occupied in the [100], [010] and [001] directions. The structure contains two nonequivalent Fe position, Fe_I and Fe_{II} of equal occupation. In each Fe position the Fe atom is situated slightly off-centre relative to the Si cube containing it. The eight Fe-Si distances are distributed in the range 2.34 - 2.39 Å for Fe_I and 2.33 - 2.44 Å for Fe_{II}. Besides, each Fe atom has two other Fe atoms at a distance of 2.97 Å. Some Mössbauer data have been published with conflicting results [16, 17, 18].

A band model has been proposed which explains the essential features of the conductivity and magnetic data available by C. BLAAUW and al [19]. The change in the character of the conduction from nonmetallic to metallic in going from β-FeSi$_2$ to α-FeSi$_2$ is in this model related to the occurence of vacancies in the Fe sublattice.
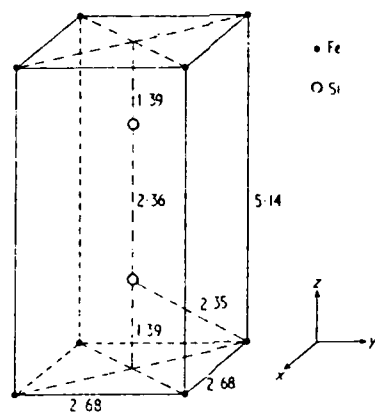

Fig. II The crystallographic unit cell of α-FeSi$_2$. Distances are given in Å The coordinate system given is referred to in the text.

I-3 CRYSTAL ELABORATION

The elaboration of single crystal of β-FeSi$_2$ was presented by WANDJI al [20], using a chemical transport by iodine. This technique is not well suited for the obtention of large size single crystals. Thus it is more interesting to use of polycrystalline materials.

The β phase of FeSi$_2$ lies at 51.3 weight % Si. By substitution of Fe by Co according to Fe$_{1-x}$Co$_x$Si$_2$ n-type samples are obtained, while substitution of Si by Al [21] or Mn [22] according to FeSi$_{2-y}$(Al or Mn)$_y$ produces p-type samples. For the preparation of specimens, silicon (99,999 %) and Iron (99,99 %) were melted together, the doping materials were added to the melt.

From the regulus samples were prepared by a ceramic technique. Hydrostatically pressed, specimens were sintered for 30 h at 1180°C (melting point 1220°C). They were then converted to β-FeSi$_2$ by annealing at 880°C for at least 24 h. For Al-doping during the process of melting and sintering, losses by Al-evaporation could not be eliminated.

II THERMOELECTRIC PROPERTIES OF β-FeSi$_2$

II-1 Intrinsic properties of FeSi$_2$:

Detailed measurements of thermoelectric power and resistivity as a function of temperature were made over the temperature range 300-900°K [11]. Fig. III and IV show the
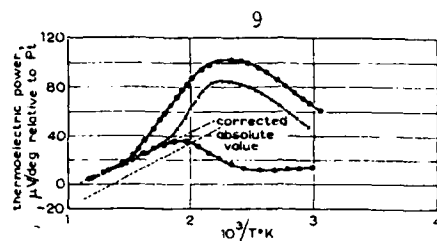
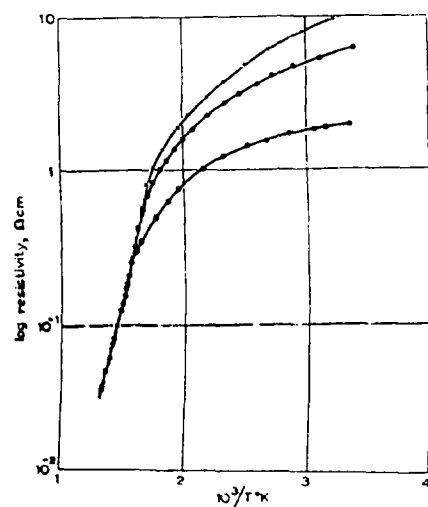Fig. III Thermoelectric power versus reciprocal temperature for $FeSi_2$.

Fig. IV Resistivity versus reciprocal temperature for $FeSi_2$.

results of measurement of thermoelectric power and resistivity as a function of reciprocal temperature. The three specimens differ slightly in impurity content. The intrinsic resistivity variation shows the exponential dependence of resistivity ρ upon $1/T$ characteristic of a semiconductor. The value of energy gap at absolute zero, Eg, calculated from the slope of the linear portion of $\log \rho/(1/T)$ curve is 0.88 ± 0.04 eV. The absolute thermoelectric power in the

intrinsic range is given by the equation :

$$\alpha = \frac{k}{e} \left[6.210^2 \left(\frac{1}{T} \right) - 8.4 \, . \, 10^{-4} \right] \mu v/deg \; C.$$

Which is in good agreement with the form of the theorical result for a simple 2-band semiconductor in the intrinsic range [23] i.e. :

$$\alpha = - \frac{k}{e} \left[\frac{b - 1}{b + 1} \frac{Eg}{2kT} + A \right]$$

$$b = mobility \; ratio \; (\mu_n/\mu_p)$$

the term A involves the appropriate scattering parameters and effective masses, and may be regarded as temperature independent. Inserting the value for Eg, obtained from the resistivity measurements, into the first term of the thermoelectric power equation gives a value for the mobility ratio of 0.8.

The upper temperature limit of a thermoelectric material is set by the value of the energy gap. Chasmar and Stratton [24] define a critical energy gap such that the production of minority carriers at the hot junction only increases the thermal conductivity by 10 % of the lattice contribution and has little effect on α (< 2 % reduction). On this basis, $FeSi_2$, with an energy gap of 0.88 eV should be suitable for use with hot junction temperatures of up to approximately 800°C.

II-2 Thermoelectric properties of doped $FeSi_2$:

It has been found possible to dope $FeSi_2$, both n and p- types. The replacement of Iron by an element to its right in the periodic table Co, Ni, or other elements from this group, produces n-type material. Substitution of a groupe III element for silicon produces p-type material.

II-2-1 Electrical conductivity and Thermoelectric power :

- n-type $FeSi_2$:

- Fig.5 shows the limits within which conductivity and thermoelectric power of p and n-$FeSi_2$ can be varied by doping. At sufficiently high doping concentrations a linear relation exists between thermoelectric power and the logarithm of conductivity [21].
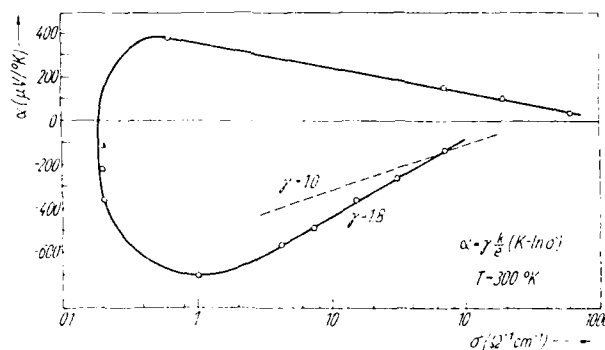

Fig. 5 Thermoelectric power of $Fe_{1-x}Co_xSi_2$ (n-type) and $FeSi_{2-y}Al_y$ (p-type) as a function of electrical conductivity

According to fig. 6 the conductivity of n-FeSi$_2$ is proportionnal to the logarithm of the doping concentration, the proportionality constant depending weakly on temperature. The conductivity of n-FeSi$_2$ shows an exponential increase in the whole temperature region (fig. 7).
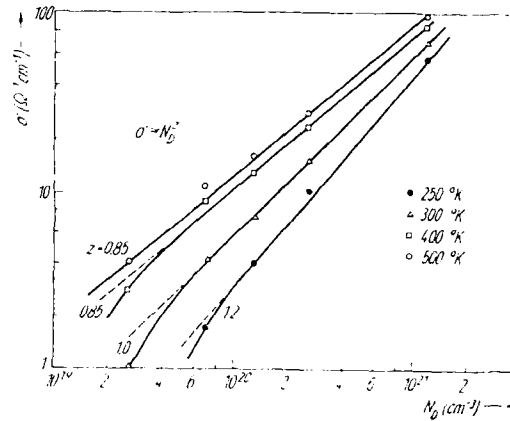

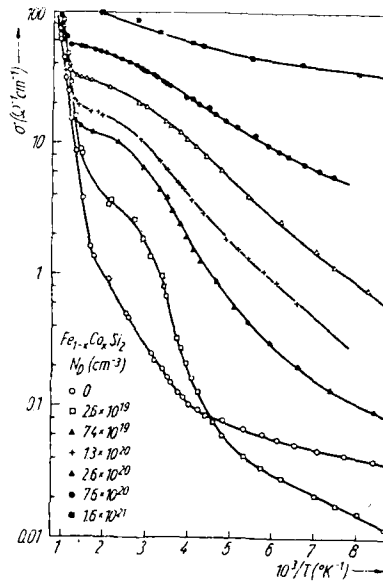Fig. 6 Conductivity of n-FeSi$_2$ as a function of doping concentration.

Fig. 7 Temperature dependence of the conductivity of n-FeSi$_2$

13

With the assumption that conduction in n-FeSi$_2$ is caused by small polarons, the mobility at room temperature is found to be $\mu_n = 0,26$ cm^2/VS.

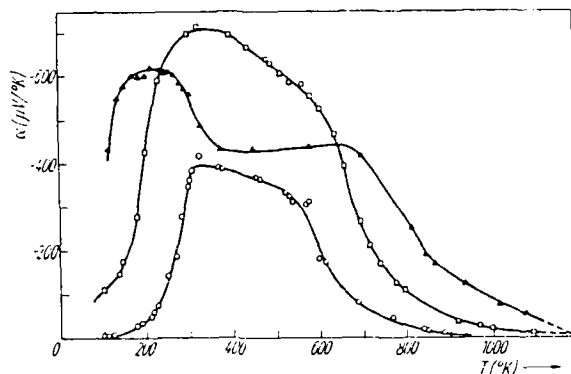The results of the measurements of thermoelectric power of n-FeSi$_2$ are shown in fig.8 - and - 9.

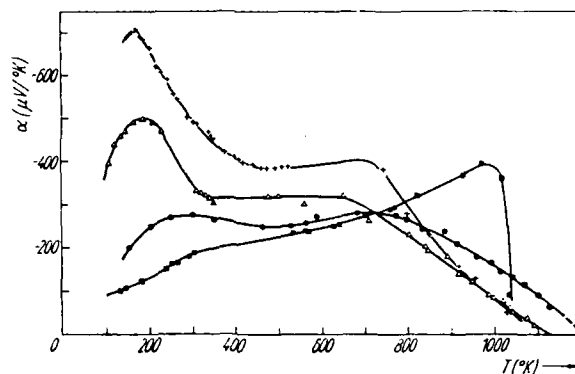Fig. 8 Temperature dependence of the thermoelectric power of weakly doped n-FeSi$_2$.

Fig. 9 Temperature dependence of the thermoelectric power of heavily doped n-FeSi$_2$

The thermoelectric power depends on temperature in a complicated way. Four regions can be distinguished. At low temperatures the thermopower increases rapidly with temperature. This can be observed most clearly for the specimens with small electron concentration (N_D = 2.6.10^{19}, 7.4.10^{19} cm^{-3}). This is probably due to the transition from impurity band conduction to polaron conduction. In the second region the thermoelectric power decreases with increasing temperature. In the third region the thermoelectric power is constant or increases slightly with temperature. This can be explained only in the polaron model because the conductivity continues to increase exponentially in this temperature region. The fourth region, in which the thermoelectric power decreases with increasing temperature corresponds to the range of intrinsic conduction.

- p-type FeSi$_2$:

The thermoelectric properties for FeSi$_2$ doped with Al or Mn (p-type) have been reported by several investigators in relation to thermoelectric conversion [11, 25, 26, 27] and the conduction mechanism could be interpreted using a band model [12, 28].

For Mn doped samples the temperature dependence of resistivity, thermoelectric power, and Hall mobility is shown in figs. 10, 11 and 12 respectively, as functions of absolute temperature [22]. As shown in fig. 10, all specimens have a semiconductor - to - metal transition with hysteresis and the jump of resistivity ρ is about one order of magnitude.

transition temperature T_C and the slope of ρ in the intrinsic region decrease with increasing Mn concentration x.

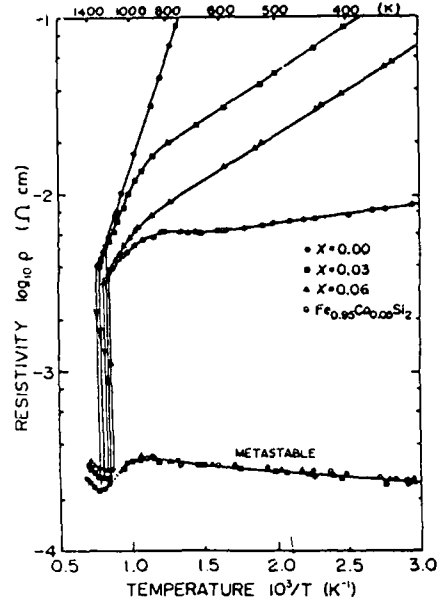Fig. 10 Temperature dependence of resistivity for p-type $Fe_{1-x}Mn_xSi_2$. Both the heating and cooling transition directions are indicated by arrows, and the open circle is n-type $FeSi_2$.
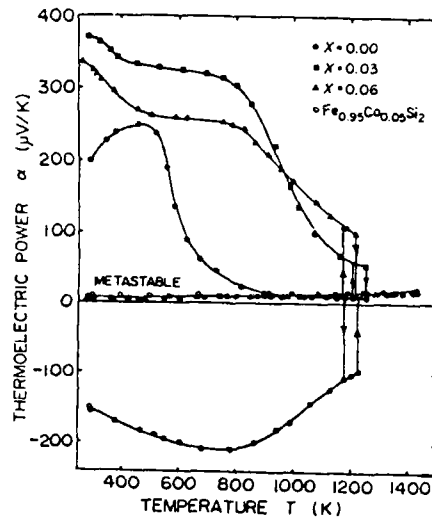

Fig. 11 Temperature dependence of thermoelectric power for p-type $Fe_{1-x}Mn_xSi_2$. Both the heating and cooling transition directions are indicated by arrows, and the open circle is p-type $FeSi_2$.

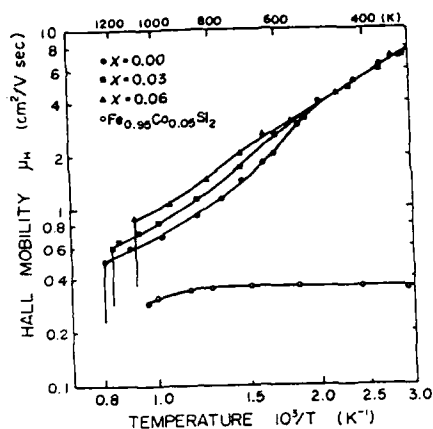Fig. 12 Temperature dependence of Hall mobility for p-type
$Fe_{1-x}Mn_xSi_2$. The open circle is n-type $FeSi_2$.

The specimens quenched from a temperature of 1100ºC are in a metastable phase with metallic conduction ; also the changes in ρ are found to be independent of x in the temperature range below 900 K. The Hall coefficient R and thermoelectric power α measurements show that the signs of the semiconducting specimens doped with Mn or Co are positive or negative, respectively, in the temperature range below T_C. The hole concentrations in $Fe_{1-x}Mn_xSi_2$ are $2.85 \ 10^{17} \ cm^{-3}$ for x = 0.00, $2.72 \ 10^{18}$ for x = 0.03 and $5.08 \ 10^{18} \ cm^{-3}$ for x = 0.06 at room temperature. The electron concentration in $Fe_{0.95}Co_{0.05}Si_2$ is $1.9 \ 10^{21} \ cm^{-3}$ at room temperature. Therefore, it was found that the Mn or Co atoms act as acceptors or donors, respectively. On the other hand, the specimens with metallic properties are whole p-type conductors and the values of α are 6-12 $\mu V/K$.

At high temperature the conductivity of the Al-doped specimens (fig 13) shows an exponential increase explained by intrinsic conduction, and at lower temperature the conductivity is proportional to $T^{-1/2}$ (fig. 14). The $T^{-1/2}$ dependence of the electrical properties of Al-doped $P - FeSi_2$ can be interpreted using the band model with a hole mobility $\mu_p \simeq 2$ cm²/VS in the region of extrinsic conduction. The temperature dependence of the thermoelectric power is shown in (fig.15). The decrease of thermoelectric power towards low temperatures may be explained by the assumption of impurity band conduction. At intermediate temperature the rise of the thermoelectric power of the sample weakly doped can be described by a log $T^{3/2}$ dependence. The temperature dependence at high temperatures is interpreted by intrinsic conduction.

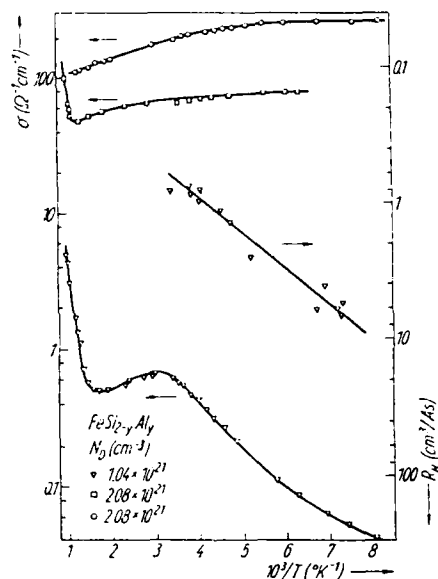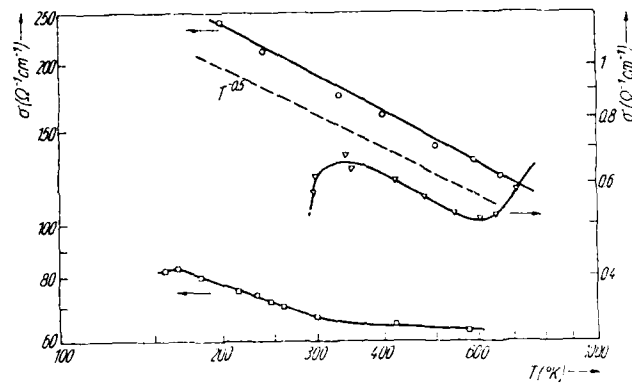Fig. 13 Temperature dependence of the conductivity and of the Hall coefficient of p-FeSi₂

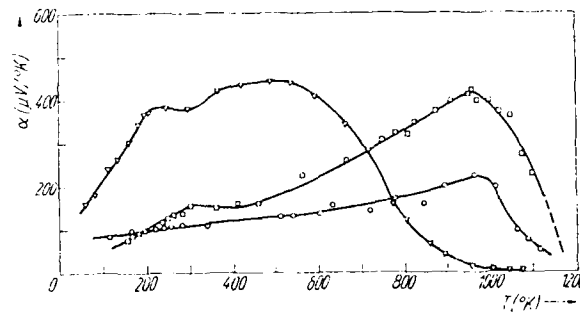Fig. 14 Conductivity of p-FeSi$_2$ as a function of temperature

Fig. 15 Temperature dependence of the thermoelectric power of p-FeSi$_2$

II-2-2 Thermal conductivity of semiconducting and metallic FeSi$_2$:

Samples prepared by a ceramic technique described before [12] have been used for the measurement of thermal

conductivity (low temperature) or thermal diffusivity (high temperatures). A summary of sample data is compiled in table.

Composition of the FeSi₂ samples

sample No. (phase)	symbol	doping concentration		composition	
		Co-atoms/cm⁻³	Al-atoms/cm⁻³	$Fe_{1-x}Co_x$ x	$Si_{2-y}Al_y$ y
3 (α)	⊤	0	0	0	0
3 (β)	○	0	0	0	0
4 (β)	∷	2.67×10^{19}	0	0.001	0
5 (β)	△	6.66×10^{19}	0	0.0025	0
6 (β)	▲	1.33×10^{20}	0	0.005	0
7 (β)	●	2.67×10^{20}	0	0.01	0
8 (β)	▽	8.00×10^{20}	0	0.03	0
9 (β)	■	1.6×10^{21}	0	0.06	0
30/5 (β)	▸	0	2.08×10^{21}	0	0.04

The thermal conductivity results for β FeSi₂ undoped and with Co doping, obtained in the temperature regime 2 to 90 K are shown in fig. (16). The electrical conductivity of semiconducting samples is sufficiently low for the electronic part of the thermal conductivity to be omitted in this regime. Therefore, the curves represent the behaviour of the lattice thermal conductivity. In the case of undoped β-FeSi₂ the thermal conductivity is proportional to T³ at very low temperature and shows a maximum near 70 K.
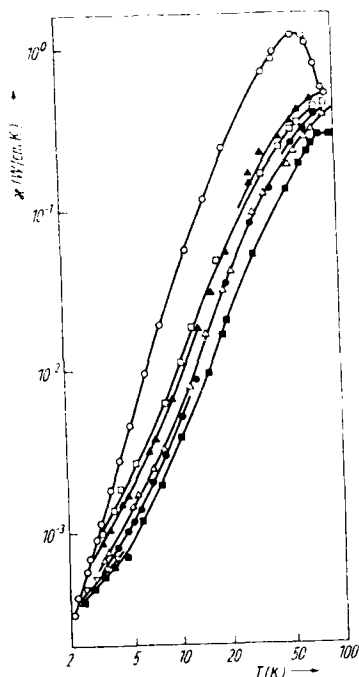

Fig. 16 Thermal conductivity of β-FeSi₂ at low temperatures (symbols as in Table)

Above 70 K the thermal conductivity is reduced by unklapp processes.

The thermal conductivity of doped samples decreases with increasing doping concentration. The total thermal resistivity should become :

$$\frac{1}{\chi} = \frac{1}{\chi_1} + \frac{1}{\chi_2} + \frac{1}{\chi_3}$$

with $\chi_1 \simeq T^3$ (crystalites), $\chi_2 \simeq T^{-1}$ (impurities [29, 30]), $\chi_3 \simeq T^2$ (dislocations [29]). By this relation the observed dependence on the doping concentration can be explained qualitatively. (For the undoped sample, boundary scattering is the dominating effect therefore $\simeq T^3$ as observed). The maxima of the thermal conductivity curves are shifted to higher temperatures with increasing doping concentration as a result of the reduced mean free path of the phonons.

At high temperature the thermal diffusivity of metallic α-FeSi$_2$ and semiconducting β-FeSi$_2$ with various doping levels in the temperature range 300 to 1300 K is shown in fig. (17). The thermal conductivities calculated by using the specific heat results of Krentsis, Maglic and Parrot [31, 32] are shown in fig. (18) as a function of temperature.
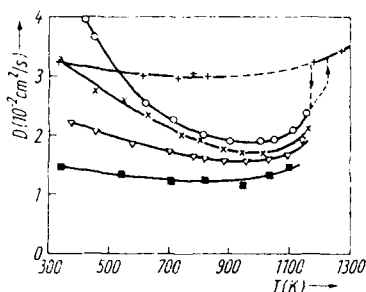

Fig. 17 Thermal diffusivity of α- and β-FeSi$_2$ at high temperatures (symbols as in table)
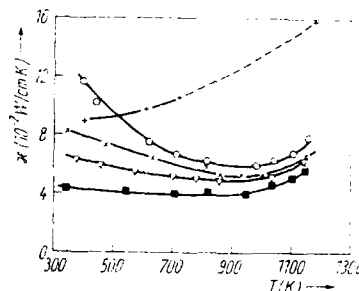
Fig. 18 Thermal conductivity of α- and β-FeSi$_2$ at high temperatures (symbols as in table)

The thermal conductivity data of β-FeSi$_2$ for high and low temperature are shown together in fig. (19). The extrinsic range (below 700 K) of all samples is characterised by a decrease of the thermal conductivity with increasing temperature. In this range the electronic part in heat conduction is negligible for the β-FeSi$_2$ samples. For undoped β-FeSi$_2$ the thermal conductivity varies as T^{-1} between 100 and 700 K. This behaviour corresponds to umklapp processes by which the phonon mean free path is limited at high temperatures.

The strong increase of the χ curves above 700 K for semiconducting FeSi$_2$ is caused by the onset of intrinsic conduction (ambipolar effect [33]).

The lattice thermal conductivity of β-FeSi$_2$ is considerably reduced as a result of doping with Aluminium or Cobalt - Some data on thermal conductivity are also obtained by Hesse [28] in a good agreement. The reduction of the thermal conductivity probably is due to point defect scattering [34, 35].
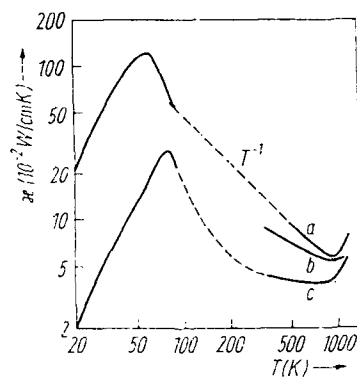
Fig. 19 Thermal conductivity of β-FeSi$_2$
(low and high temperatures) ; (a) undoped,
(b) 2.1 x 10^{21} cm^{-3} Al, (c) 1.6 x 10^{21} cm^{-3} Co.

II-2-3 <u>Figure of merit of doped β-FeSi$_2$ - Discussion</u> :

Fig. (20) shows the variation of the figure of merit with temperature for an FeSi$_2$-FeAl$_2$ p-type material and an FeSi$_2$-CoSi$_2$ n-type material. These values of Z were calculated on the assumption that thermal conductivity is constant and equal to 0.04 Watt units. Since χ should decrease with temperature, the values of Z are probably pessimistic.
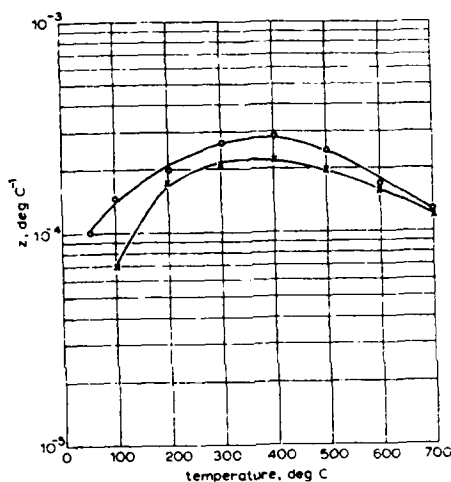
Fig. 20 Figure of merit of n- and p-type FeSi$_2$.
O FeSi$_2$-5 % CoSi$_2$ n-type.
x FeSi$_2$-2 % FeAl$_2$ p-type.

More over the technique of elaboration presents no special difficulties and seems to have a low cost. But the time needed for the phase transition from the metallic high temperature to the semiconducting phase is found to be very sensitive to the stoichiometric composition of the material [36]. An other problem is also due to the low solubility of Al - doping, and a part of this one is lost by evaporation during

sintering, then the doping concentration is not exactly known.

It is necessary to perform the annealing process under high vacuum in order to avoid aluminium oxidation. The n-type material and p-type with Manganese-doping, however, seem to be insensible to the annealing atmosphere.

Iron disilicide is oxidation-resistant and thermally stable over the full range of operating temperature 150-650°C. Encapsulation is therefore unnecessary. Since the material can be doped both n and p-type, both legs of the thermocouple can be constructed of the same basic materials, thus elimating problems of differential thermal expansion. A further advantage of this material is the high level of doping required for optimization of thermoelectric properties. This means that high-purity materials are not required, and the diffusion of small amounts of impurities into the elements during operation will not cause degradation of thermoelectric properties. Since Iron and Silicon are both cheap and plenti ful, the material cost of the generator will be low. Nevertheless in the range of 700-800°C for the hot function the problem of diffusion and oxidation has to be considered [36].

III NEW AMORPHOUS MATERIAL FeSi$_2$

Amorphous films of Iron disilicide FeSi$_2$, prepared by ionized cluster beam (ICB) deposition [37, 38] has been investigated to develop a new power source device for energy conversion [39]. High purity iron and Silicon (or silicon mono

oxide) were used as source materials, and were heated at 1800°C for Fe and 2000°C for Si in two confinement crucibles.

Aggregate (clusters) of atoms held together by weak forces are formed as a result of adiabatic expansion through a nozzle, which consist of approximately 1000 individual atoms. Two cluster beams of Fe and Si ejected from each crucible are independently ionized by electron impacts, and accelerated toward a substrate. Films were deposited in an oxygen particle pressure $10^{-3} \simeq 10^{-4}$ Torr on fused silica substrates heated at about 300°C.

As deposited $FeSi_2$ films were found to show typical amorphous structure. Fig. 21 shows the temperature dependence of Seebeck coefficient obtained for amorphous Fe-Si films with a composition ranging from 50 to 83 atom % Si.
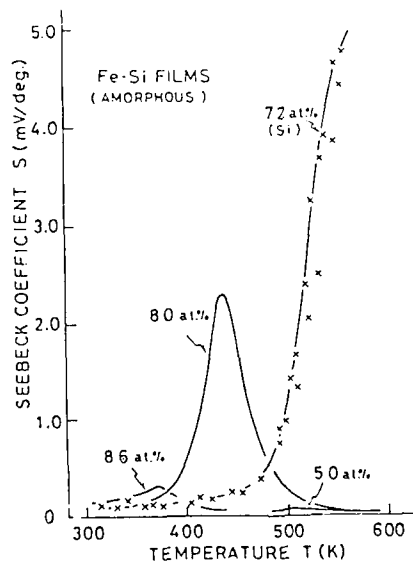

Fig. 21 Temperature dependence of the Seebeck coefficient α for amorphous Fe-Si films with different compositions of Si.

The value of α for FeSi (50 at % Si), which was metallic, was as low as 40 μV/deg., while for $FeSi_2$ (72 at % Si) the extremely high value of α $\simeq$ 5 mV/deg. was obtained at about 550 K. Therfore, the giant thermoelectric power for $FeSi_2$ film can be considered to be caused by dominant Si-O pair boudings. Beyond the composition of $FeSi_2$ phase, the thermoelectric power considerably decreased, and the peak values of α was found to shift toward lower temperature side with an increase of Si content. These Fe-Si amorphous films were deposited by activated reaction of ionized Si-clusters with oxygen. Fig. 22 shows the Seebeck coefficient as a function of temperature for a n-type film obtained when Fe-clusters were only ionized in a 10^{-4} Torr oxygen. Substition of 3d-transition metals (Mn, Cr, Co, Ni) for Fe was investigated over a wide range of doping. The effect of Mn substitution on the thermoelectric power is shown in Fig. 23. It is found that the optimum thermoelectric properties are for~ ` by the suitable doping of manganese (0,5 at % Mn) for ℙ-type conduction.
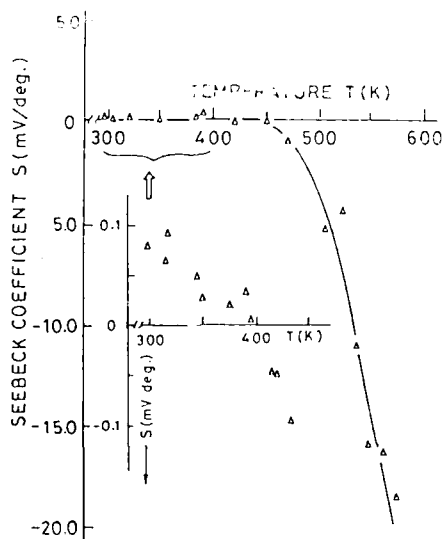
Fig. 22 Temperature dependence of the Seebeck coefficient α for a $FeSi_2$ amorphous film.
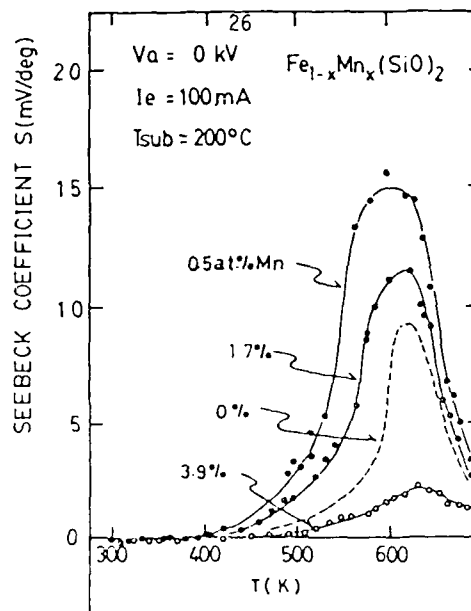
Fig. 23 Temperature dependence of the Seebeck coefficient α for $Fe_{1-x}Mn_x(SiO)_2$ amorphous films.

The electrical conductivity σ of these amorphous films are shown in fig. 24. The film doped with 0,5 at % Mn (α_{max}) is found to have a lower conductivity compared with the other films but higher than that of non doped films.
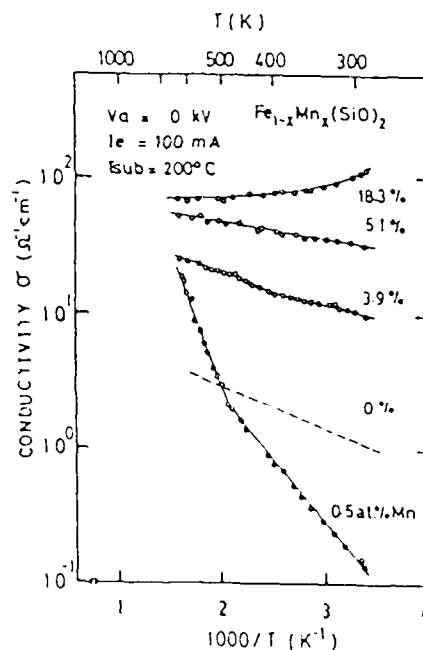
Fig. 24 Temperature dependence of the electrical conductivity σ for $Fe_{1-x}Mn_x(SiO)_2$ amorphous films.

The effect of Cr substitution on the thermoelectric properties is shown in fig. 25 and 26 over up to 1300 K, but exibits a change in conductivity at 450 K.

Finally a higher figure of merit Z, is reported by Matsubara [40, 41], assuming thermal conductivity to be equal to $1 \, W.m^{-1}.K^{-1}$.

Another structural and electrical investigations are made on amorphous material $FeSi_2$, showing recrystallization of $FeSi_2$ films by thermal heating [42, 43].

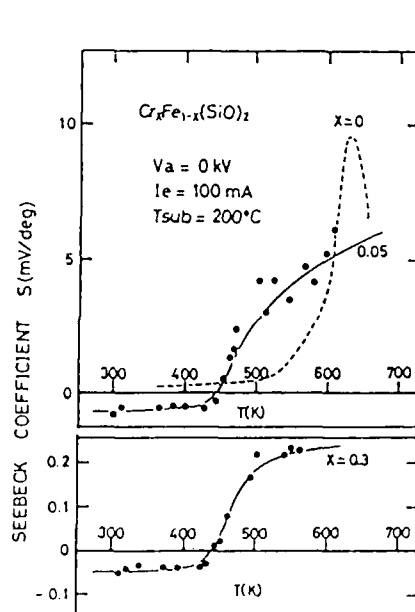Fig. 25 Temperature dependence of the Seebeck coefficient α for $Cr_xFe_{1-x}(SiO)_2$ amorphous films.
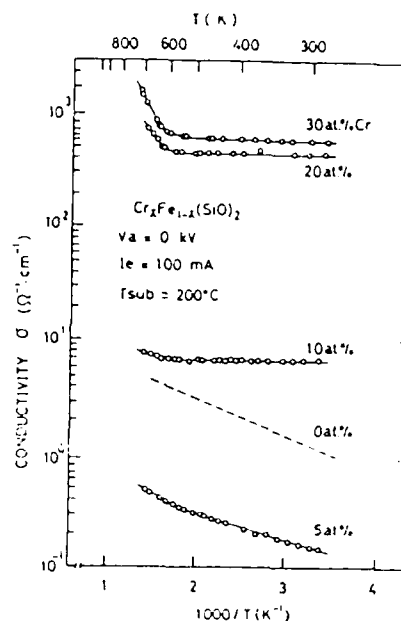
Fig. 26 Temperature dependence of the electrical conductivity for $Cr_xFe_{1-x}(SiO)_2$ amorphous films.

IV CONCLUSION

Iron disilicide is a semiconductor with an energy gap of 0.88 ± 0.04 eV. It can be doped n or p-type by the addition of appropriate impurities and optimum doping yields to thermoelectric material with $Z = 2.10^{-4}$ K^{-1} over the temperature range 150 - 800°C. But at higher temperatures some problems come into sight ; at the hot junction the contacts are not easy to perfom and interdiffusion of doping elements can perturbe this one.Its figure of merit is not so high as Bi-Te type materials but it has the eminent advantage that the highest service temperature is much higher than Bi-Te.

Some advantages of β-FeSi$_2$ are also of considerable interest : the compound is very cheap ; the material exibits good thermal and mechanical properties.

When the material is amorphous (always thin films) it presents a very large figure of merit $Z = 10^{-3}$ K^{-1}; but this one was calculated and not measured because it was very difficult to measure the thermal conductivity on thin films. Oth erwise at higher temperature above 400 °C ,the amorphous films must recrystallize and become a metallic phase.

REFERENCES

1   N.K. ABRIKOSOV. IZV. Sekt. Fiz. Khim. analiza 27.157 (1956).

2   I.N. STRUKOV and P.V. GELD. Fiz. Metallov i Metallovedenie 4. 190 (1957).

3   F.A. SIDORENKO. P.V. GELD, and L.B. DUBROVSKAYA, Fiz. Metallov i Metallovedenie 8, 465 (1959).

4   J.P. PITON and M.F. FAY, C.R. Acad. Sci. C 266, 154 (1968).

5   J. VAN DEN BOOMCAARD J. Iron Steel Inst. 210(4) - 276 (1972)

6   N.K. ABRIKOSOV. Bull. Acad. Sci. USSR 21, 137 (1957).

7   K. WEFERS, Metall 17. 446 (1963).

8   F.A. SIDORENKO, P.V. GELD, and M.A. SHUMILOV. Fiz. Metallov i Metallovedenie 9. 861 (1960).

9   I.N. STRUKOV and P.V. GELD, Fiz. Metallov i Metallovedenie 3. 564 (1956).

10 R. BUCKSCH. Z. Naturf. 22a, 2124 (1967).

11 R.M. WARE and D.J. MC NEILL Proc. IEE 111 178 (1964).

12 U. BIRKHOLZ and A. FRÜHAUF A Phys. Stat. Solidi 34 K181-4 (1969).

13 Y. DUSAUSOY. J. PROTAS. R. WANDJI and B. ROQUES Acta Crystallogr 27 1209-18 (1971).

14 C. LE CORRE and J.M. GENIN Phys. Stat. Solidi 51 K85-8 (1972).

15 F.A. SIDORENKO. P.V. GEL'D and L.B. DUBROVSKAYA Fiz. metal. metalloved. 8 735-9 (1959).

16 R. WAPPLING. L.HAGGSTRÖM and S. RUNDQVIST Chem. Phys. Lett. 2 160-1 (1968).

17 I.A. DUBOVTEV and F.A. SIDORENKO. JETP Lett. 14 134-5 (1971).

18 R. WANDJI. C. LE CORRE. J.M. GENIN and B. ROQUES Phys. Stat. Solidi (b) 45 K123-7 (1971).

19 C. BLAAUW. F. VAN DER WOUDE and G.A. SAWATZKY, J. Phys. 6-2371 (1973).

20 R. WANDJI, Y. DUSAUSOY, J. PROTAS, B. ROQUES CRAS 267. 1587-90 (1968).

21 U. BIRKHOLZ, J. SCHELM Phys. Stat. Sol. 27, 413 (1968).

22 I. NISHIDA, Phys. Rev. 7, 2710-13 (1973).

23   TAUC : Photo and Thermoelectric effects in semiconductors (Pergamon, 1962).

24   R.P. CHASMAR, R. STRATTON, J. Electr. Control 1,52 (1959).

25   G.V. SAMSONOVE, Refractory Transition Metal Compound, transl. by
      G.E. GURR and D.J. PARKER p. 178 (Academic N.Y. 1955).

26   J. HESSE, Z. Angew. Phys. 28, 133 (1969).

27   J. HESSE and R. BUCKSH, J. Mater. Sci. 5, 272 (1970).

28   J. HESSE, Z. Metallkd. 60, 652 (1969).

29   P.G. KLEMENS Proc. Roy. Soc. A 208, 108 (1951).

30   J.M. ZIMAN Canad. J. Phys. 34, 1256 (1956).

31   P.G. KRENTSIS, P.V. GELD and G.I. KALISHEVITCH, Tchernaja Metallur-
      giya 11, 146 (1963).

32   K. MAGLIC and J.E. PARROT Vundesministerium für Bildung und
      Wissenschaft, Forschungsbericht K 70-01 (1970).

33   P.J. PRICE Phil. Mag. 46, 1252 (1955).

34   B. ABELES Phys. Rev. 131, 1906 (1963).

35   P.G. KLEMENS Proc. Phys. Soc. 68, 1113 (1955).

36   U. STÖHRER, R. VOGGESBERGER, G. WAGNER and U. BIRKHOLZ,
      Proc. 1st Europ. Conf. on Therm., Cardiff (1987).

37   T. TAKAGI, I. YAMADA, M. KUNORI and S. KOBIYAMA, Proc. 2nd Int.
      Conf. on Ion Source (Vienna, Austria), p. 790, sept.. (1972).

38   T. TAKAGI, K. MATSUBARA, H. TAKAOKA and I. YAMADA, Thin
      Solid Films, 63, 41 (1979).

39   T. TAKAGI, K. MATSUBARA, M. OURA and T. KOYANAGI, Proc. 6th
      Symp. on Sour. and Ion-Assist. Technol. (Tokyo), 1982 (IEEJ, Tokyo), p. 391,
      Jun, (1982).

40   K. MATSUBARA, H. KUNO, Y. OKUNO, H. TAKAOKA and
      T. TAKAGI, Proc. Int. Ion Eng. Congress - ISIAT 83 KYOTO (1983).

41   K. MATSUBARA, T. KOYANAGI, T. TAGAKI, Proc. 6th ICTEC Arlington
      Texas (1986).

42   H.P. GESERICH, S.K. SHARMA, and W.A. THEINER, PHIL. MAG. 27-4,
      10001-07 (1973).

43   KAMNA AGGARWAL and R.G. MENDIRATTA, Phys. Stat. Sol. (A) 53,
      K95 (1979).

SECOND PART

THERMAL FLUX PROTOTYPE

SUMMARY

SECOND PART : THERMAL FLUX PROTOTYPE

INTRODUCTION

Iron disilicide couples are used in Japan to generate very small electrical powers for the controls of gas heaters.

KOMATSU ELECTRONICS Ltd commercializes these couples.

They supply the electrical and thermal characteristics as a function of temperature.

From these characteristics, one can calculate the efficiency : ratio of electrical power to thermal power.

These couple are very well suited for operation in an oxydizing flame because the silicon becomes SiO_2 (quartz) which is an excellent protector. This layer automatically regenerates itself in the presence of oxygen.

It is nearly impossible to measure heat fluxes, if the hot junction is in a flame.

OBJECTIVE AND CONCLUSIONS

The object of this study is to build a small prototype where the heat source is a metal at a known temperature heated by an electrical heater with a measurable power (V, I).

The unit was operated without any couples and then with couples. The heating power was measured for both cases (with and without couples) keeping the surface temperature of the heat source constant. In steady state conditions the difference in powers between the case with and without couples represents the heat going through the couples.

Simultaneously the electrical parameters of the couples were measured.

The efficiency is defined as the ratio of the electrical power to the thermal power going through the couples.

The measured efficiency of the couples with the hot junction at 720°C was found to be : 0.87 %, while Komatsu's value was 0.63 %. With 18 couples in series the total voltage is 2.5 V and the wattage is 0.75 W.

SUMMARY

The couples manufactured by Komatsu are described and manufacturer's characteristics are given in Chapter 1.

A description of the experimental arrangement is given in Chapter 2.

The experiments are given in Chapter 3, which includes a description of the experimental procedure, the experimental results and the analysis of results.

The Chapter 4 covers the experimental results, the comparaison between the predicted performances and those that have been measured.

Comparisons with a material made by the University of Karlsruhe are presented in Chapter 5.

A small prototype of a generator with a flame is presented with its performances in Chapter 6.

1 - IRON DISILICIDE COUPLES

Iron disilicide couples manufactured by KOMATSU ELECTRONICS Ltd are presented.

Two photographs of a couple (top views and side view) are given page with its geometric dimensions Fig. 1.1.

The Seebeck values for N and P are given in Fig. 1.2. The thermal conductivity for N and P is given in Fig. 1.3.

The electrical characteristics are given in Fig. 1.4 which include the overall resistance of each couple.

It has turns out to be useful to numerize KOMATSU'S curves. The numerical values are presented in table 1.1.

The effective Seebeck is N + P.

In the case of thermal conductivity, one can consider the value of $\frac{N + P}{2}$, because the two types are thermally in parallel.

In table 1.2 for the couple performances (top table) the last two columns are calculated from the values given by KOMATSU.

In the bottom table the figure of merit is calculated.

Tm is the average temperature of the couple.

Using these values we will in Chapter 4 compare the experimental results to the calculed ones.
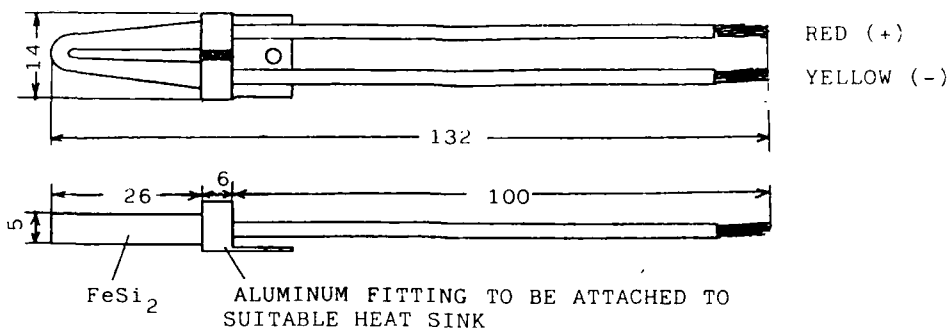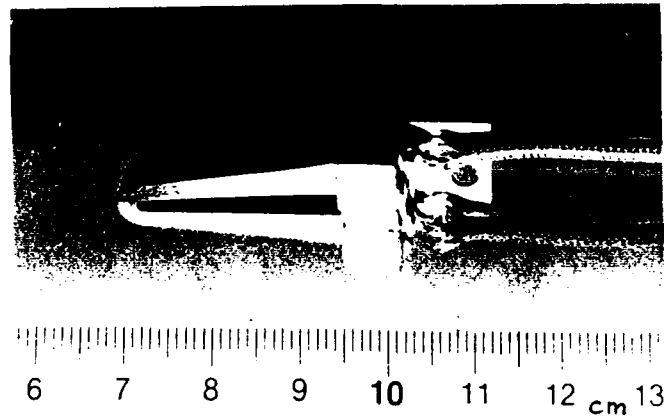
RED (+)

YELLOW (-)

14

132

26   6   100

5

FeSi$_2$ ALUMINUM FITTING TO BE ATTACHED TO
SUITABLE HEAT SINK

Fig. 1.1   IRON DISILICIDE THERMOELECTRIC COUPLE

KOMATSU ELECTRONICS INC.

IRON DISILICIDE THERMOELECTRIC COUPLE

KOMATSU ELECTRONICS INC.

Fig. 1.2 - Seebeck coefficient

IRON DISILICIDE THERMOELECTRIC COUPLE
KOMATSU ELECTRONICS INC.

Fig. 1.3 THERMAL CONDUCTIVITY OF FeSi$_2$

IRON DISILICIDE THERMOELECTRIC COUPLE

KOMATSU ELECTRONICS INC.
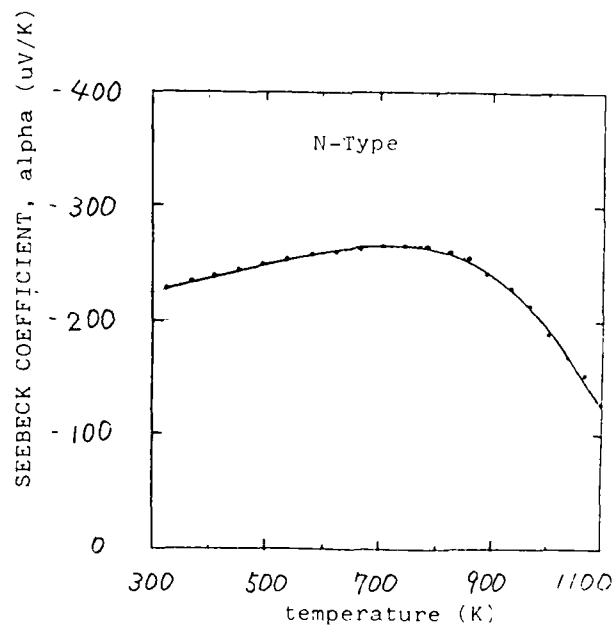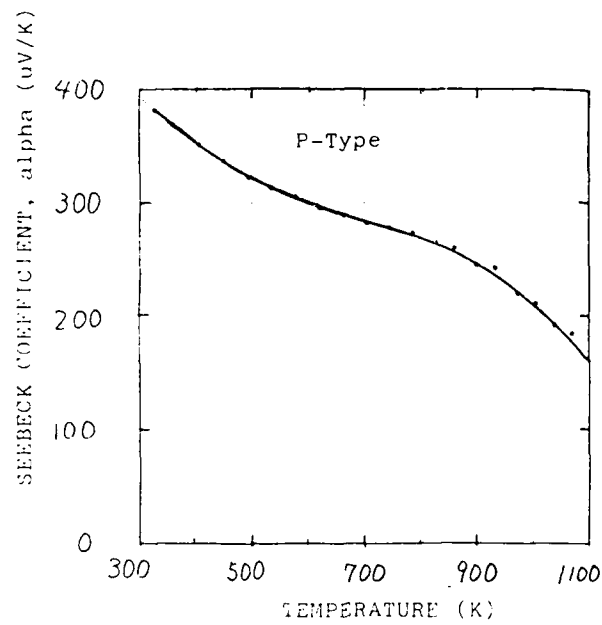
COURTESY KOMATSU ELECTRONICS LTD
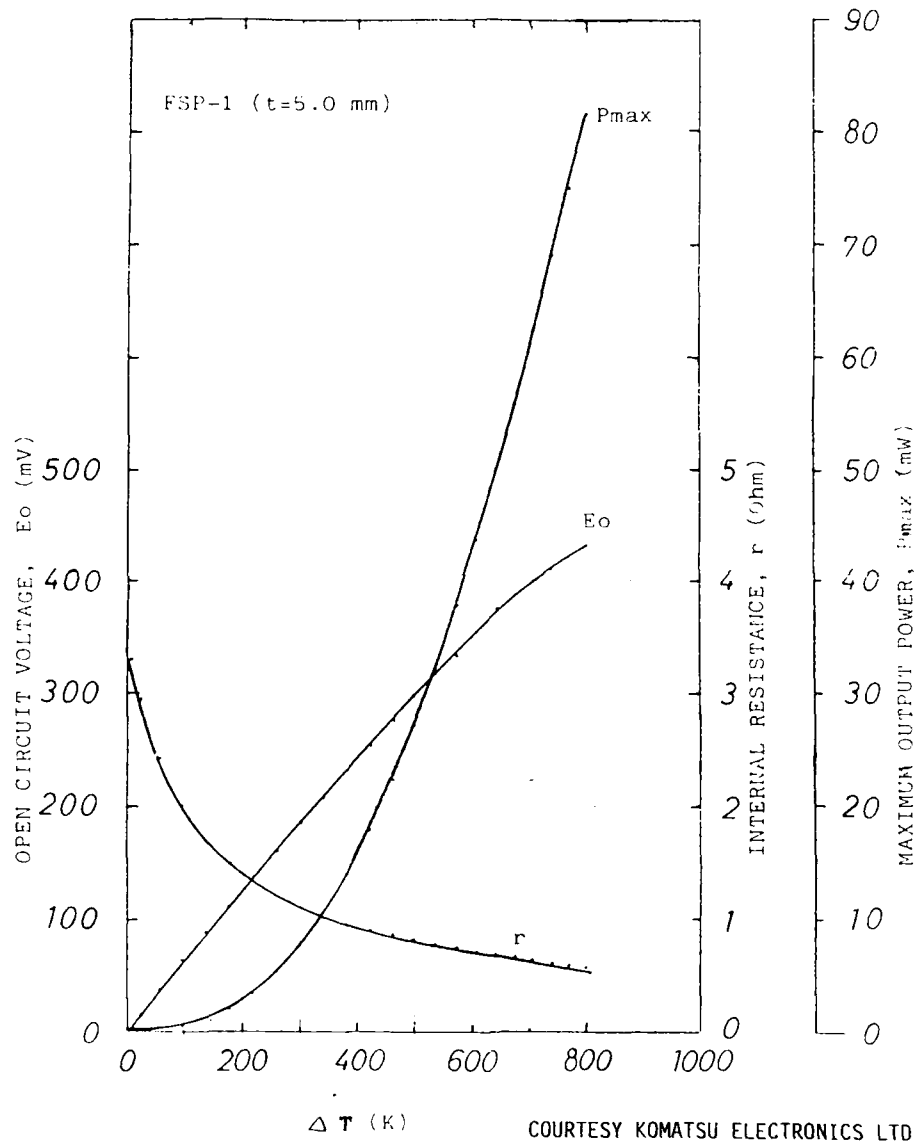
Fig. 1.4 - Electrical characteristics

IRON DISILICIDE THERMOELECTRIC COUPLE

KOMATSU ELECTRONICS INC.

Numerization from curves supplied by KOMATSU ELECTRONICS LTD

CHARACTERISTICS

Seebeck Coefficient µV/K

T	t	N type	P type	N+P	$\frac{N+P}{2}$
K	°C				
300	27	225	390	615	307.5
400	127	235	352	587	293.5
500	227	250	323	573	286.5
600	327	256	300	556	278
700	427	265	283	548	274
800	527	262	268	530	265
900	627	240	245	485	242.5
1000	727	195	207	402	201
1100	827	125	160	285	142.5

Thermal Conductivity W/(m.K)

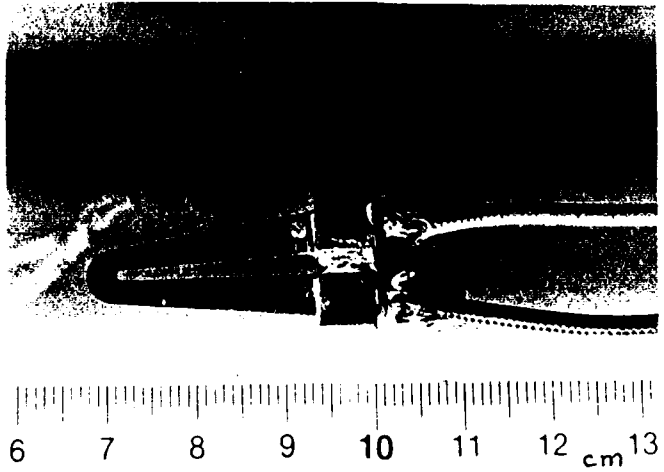| t °C	P type	N type	$\frac{N+P}{2}$
0	20.5	11.7	16.1
100	13.5	10.2	11.85
200	11.4	9.0	10.2
300	10.2	8.1	9.15
400	9.2	7.4	8.3
500	8.4	6.8	7.6
600	7.8	6.4	7.1
700	7.3	6.0	6.65
800	6.9	5.8	6.35

Table 1.1 - NUMERICAL VALUES TAKEN FROM

FIGURES 1.2 and 1.3

KOMATSU ELECTRONICS INC.

Couple performances

ΔT	r couple	P max $(r=R_L)$	Open-circuit Voltage	Voltage with $R_L=r$ $v=\sqrt{r \cdot P \; max}$	Current $I=\sqrt{P \; max/r}$
K	Ω	mW	mV	mV	mA
0	3.25	0	0		
100	1.95	0.5	55	31	11
200	1.38	2.7	122	61	38
300	1.08	7.5	180	90	83
400	0.90	15.3	240	117	131
500	0.80	27	295	147	184
600	0.70	42	345	171	246
700	0.60	60	390	190	316
800	0.53	80.5	425	206	391

Resistivity

Cross section :

$$S = \frac{2.5 \times 5 + 4.5 \times 5}{2} = 17.5 \; mm^2$$

$$\ell = 2 \times 31 \; mm$$

$$\rho = R \times \frac{S}{\ell} = R \times 2.8226 . 10^{-4} \; \Omega m$$

ΔT	$Tav=30+\frac{\Delta T}{2}(^\circ c)$	R	ρ	average Seebeck $\frac{N+P}{2}$	Thermal conductivity W/(m-K)			Figure of merit *
K	$^\circ$C	K	Ω	$\mu \Omega m$	μV /K	P	N	$\frac{N+P}{2}$	10^{4}K
0	30	303	3.25	917.3	307	18.40	11.25	14.82	0.07
100	80	353	1.95	550.4	297	13.90	10.50	12.20	0.13
200	130	403	1.38	389.5	294	13.17	9.84	11.51	0.19
300	180	453	1.08	304.8	290	11.82	9.24	10.53	0.26
400	230	503	0.90	254.0	287	11.04	8.73	9.88	0.33
500	280	553	0.80	225.8	280	10.42	8.28	9.35	0.37
600	330	603	0.70	197.6	273	9.90	7.89	8.90	0.43
700	380	653	0.60	169.4	274	9.40	7.54	8.47	0.52
800	430	703	0.53	149.6	274	8.96	7.22	8.09	0.62

* The figure of merit of the material is calculated using the
average values $(\frac{N + P}{2})$ for Seebeck, resistivity and thermal
conductivity.

Table 1.2 - NUMERICAL VALUES TAKEN FROM

FIGURE 1.4

IRON DISILICIDE

$FeSi_2$

KOMATSU ELECTRONICS INC.
THERMOELECTRICS·ELECTRONIC EQUIPMENTS

SALES: 2597 SHINOMIYA,HIRATSUKA-SHI,KANAGAWA-KEN,JAPAN.
         TEL.0463-23-7561   FAX.0463-23-7022
         TELEX.3882-429 KOMATU J
KANSAI
 OFFICE: 17 TAKADA,MORIMOTO-CHO,MUKO-SHI,KYOTO-FU,JAPAN.
         TEL.075-922-3385   FAX.075-932-3334
FACTORY: 2597 SHINOMIYA,HIRATSUKA-SHI,KANAGAWA-KEN,JAPAN.

KOMATSU THERMOELECTRIC

In 1957, Research Section of the Komatsu Ltd. started research and development on the thermoelectric semiconductors and their application.

In 1960, the Komatsu Electronics Inc., a subsidialy company of the Komatsu Ltd. was established and started the manufacture and sales business of the thermomodules and the apparatus using them.

In 1983, the Komatsu Electronics Inc. has evolved a fablication technology of the Iron Disilicide Thermoelements, using a great fund of thermoelectric experience, for the thermoelectric electricity generating at high temperature, under the licence of the Japan PAT. 1977-47677 of the National Research Institute for Metals, Tokyo, Japan.

1. PRINCIPLE

Photo. 1

P-N Junction — Heat

FeSi$_2$ (P-Type)

FeSi$_2$ (N-Type) ΔT

Cool

Load (Power)
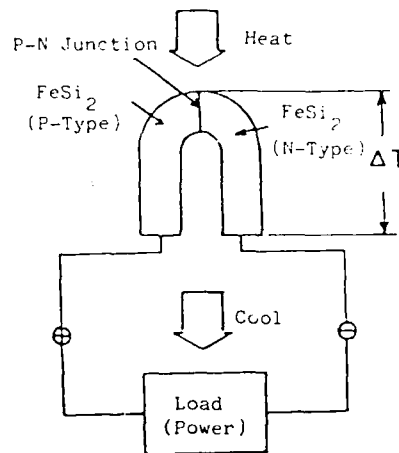
Fig. 1

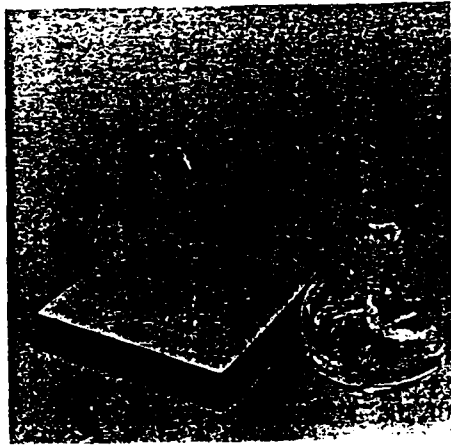 The most basic form of Thermoelectric Electricity Generating Device is shown in Fig. 1.

 When the P-N Junction is heated and the othersides cooled, negative charge is generated in the "N"-Type coldside, and positive charge in the "P"-Type coldside. If the outer load is connected between the coldside electrodes, electric power can be taken from this device.

 The most simple demonstration is shown in Photo. 1.

Cement

FeSi$_2$ Thermoelement

Covered Wire (Heat Proof) { Wire Dia. : 3.5 mm / Cable Dia. : 1.4 mm / Number of Cable: 48

Red (+)

Black (-)
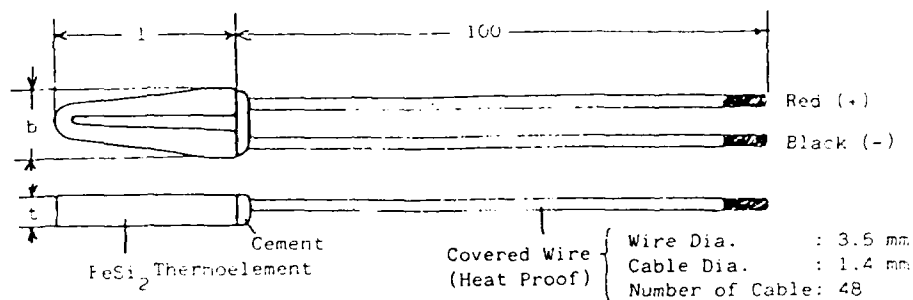
SPECIFICATION CHART

	Output Voltage E o(V)	Electric. Resistance r (Ohm)	Max. Power Pmax (mW)	Size		
				l(mm)	b(mm)	t(mm)
FSC-1 (Sensor-Type)	0.49	1.60	37	31	11	3
FSP-1 (Power-Type)	0.36	0.34	95	31	11	5.7

Under the condition: Hot Junction Temperature=830 $^{\circ}$C
Cold Junction Temperature=30 $^{\circ}$C
E=Open Circuit Voltage (V)
$r=R_L$　　(r=Internal Resistance, R_L=Load Resistance)

3. ALLOWABLE TEMPERATURE RANGE

Allowable P-N Junction Temperature: 830 $^{\circ}$C (not continuous)
800 $^{\circ}$C (continuous)

Allowable Coldside Temperature: below 400 $^{\circ}$C

4. CHARACTERISTIC CURVE

1) Output Power vs Temperature Difference (for Sensor-Type FSC-1)
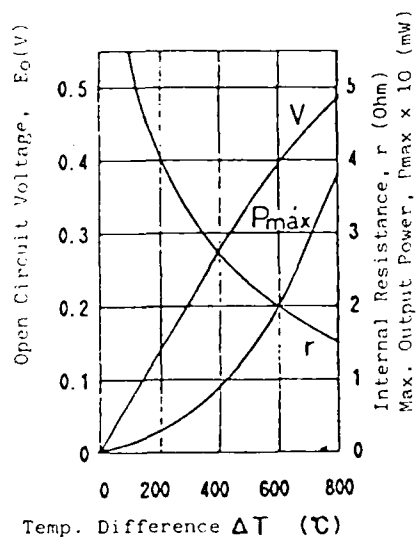
(a) Coldside Water Cooled
(Tc=30 $^{\circ}$C Const)
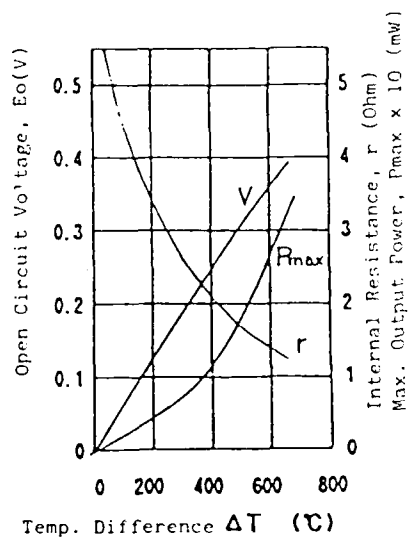
(b) Coldside Air Cooled
(Tc=200 $^{\circ}$C)

Fig. 2

2) Load Characteristic Curve (for Power-Type FSP-1)

Equivalent Circuit

Fig. 3

Electric Current (Amps)
at Temp. Difference=800 $^{\circ}$C
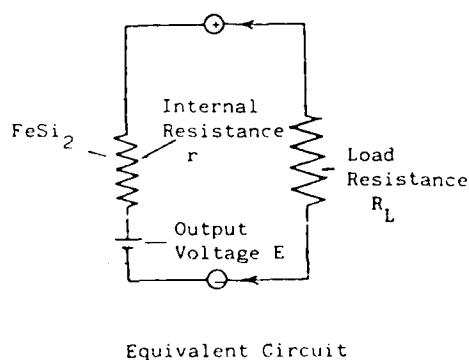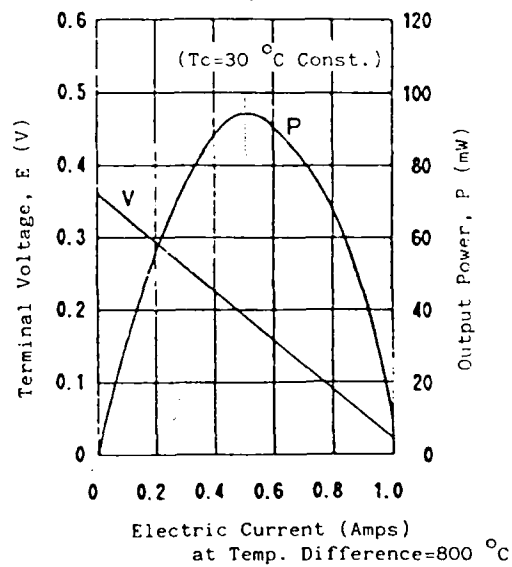
Fig. 4

- 4 -

5. NOTE FOR HANDLING

1) Mechanical Precautions

Because Iron Disilicide $FeSi_2$ is a powder metallugical semi-conductor, don't give a shock by dropping or beating. (see Fig. 5)

Drop!

Beat!
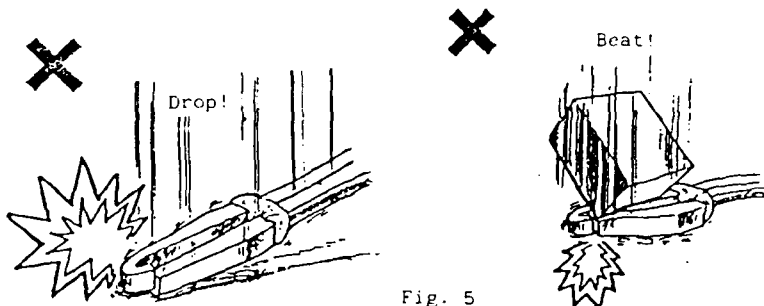
Fig. 5

Don't give force directed by arrws showing in Fig. 6.

(a) PULL   (b) PUSH

Force   Force   Force   Force
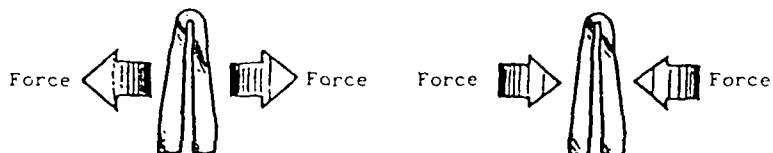
Fig. 6

Don't give a mechanical stress at junctions between $FeSi_2$ and lead wires, when bending the leadwires. (see Fig. 7)
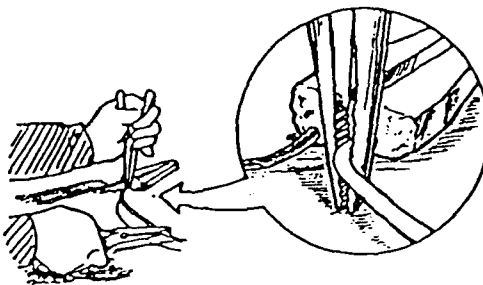
Fig. 7

6. HOW TO USE

When heating the hotside P-N Junction by flame, thermoelement should be exposed to flame within 10 mm from the top of P-N Junction, in order to keep temperature difference between hot and coldside. (see Fig. 8)
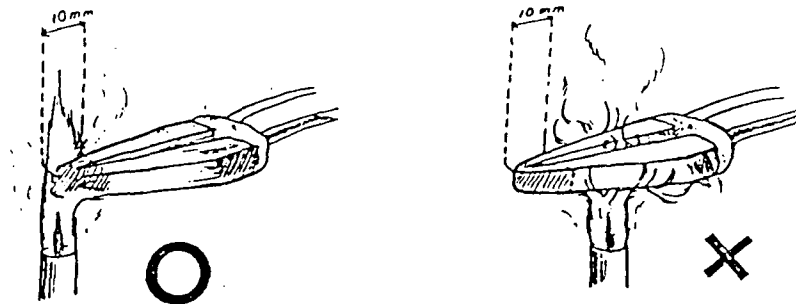
Fig. 8

The highest limit of the hotside temperature Th is 830 $^\circ$C, when cotinuous running it is advisable to keep below 800 $^\circ$C.

Attach the suitable heat dissipator at coldsides of the thermoelement, in order to keep the temperature difference between hot and coldside.(see Fig.9)

Heat Dissipator
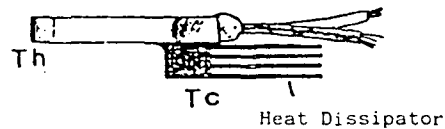
$$Th \leq 800\,^\circ C$$
$$Tc < 200\,^\circ C$$

Fig. 9

Don't splash water on the thermoelement when heating or right after heating, otherwise the thermoelement might be broken by thermal shock.

(see Fig. 10)
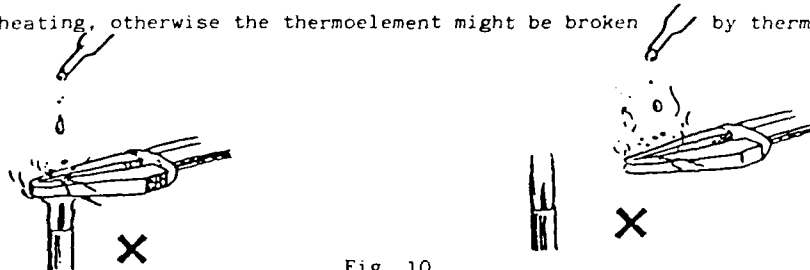
Fig. 10

7. FEATURES

1) Iron Disilicide $FeSi_2$ is possible to use at high temperature (800 $^{\circ}C$) exposed in air.

2) Low cost compared with other thermoelectric alloys.

3) Output voltage is 15 times larger than metalic thermo-couples.

4) No moving parts, no noise, no vibration, no ware, no maintenance.

8. APPLICATION

1) Power source for automatic temperature controller of gas equipment.

2) Temperature sensor for safety device of gas equipment.

3) Cordless forced air heating system.

4) Noiseless power source for electronic equipment using exaust heat from combustion engine.

5) Power source for unmanned meteorogical observatory, lighthouse or communication.

6) Emergency power source.

THERMAL CONDUCTIVITY OF FeSi$_2$
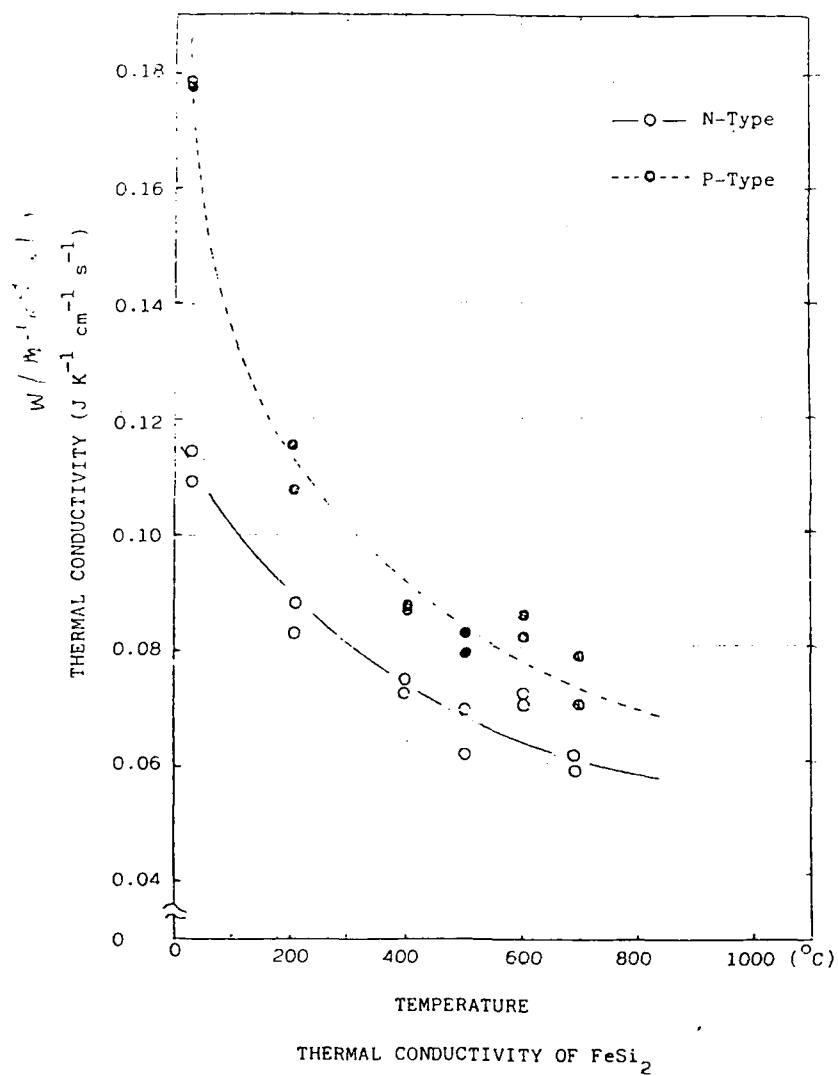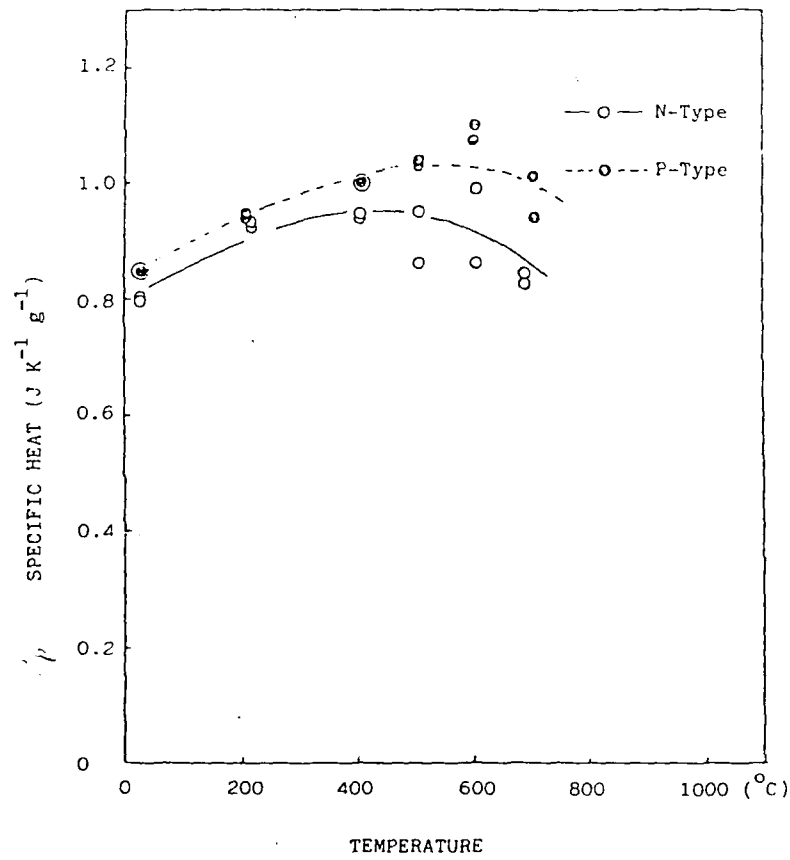
SPECIFIC HEAT OF $FeSi_2$
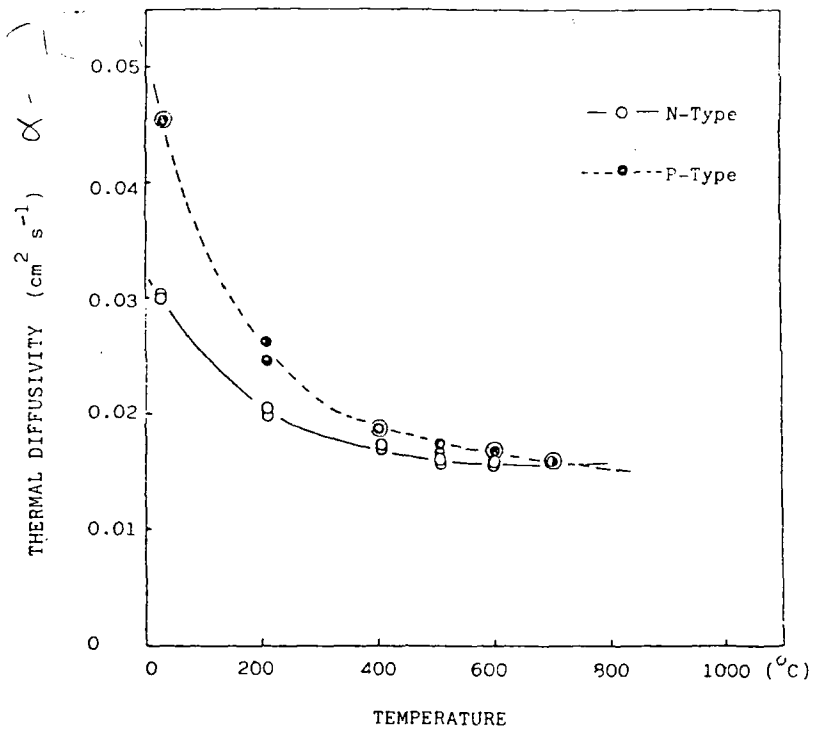
THERMAL DIFFUSIVITY OF FeSi$_2$

2 – DESCRIPTION OF EXPERIMENTAL ARRANGEMENT

The experimental arrangement is composed of :

- a hot source and a heat sink that constitue a temperature
  differential unit
- the power supply for the hot source
- the external load circuit

with the adapted instrumentation for measuring the required
values and to collect the data.

2.1. Temperature differential unit (thermal flux prototype

This unit comprises the hot source and the heat sink which are
needed at the hot and the cold junctions of the thermoelectric
couples.

The protographs Fig. 2.1 and 2.2 show the unit and the drawing
Fig. 2.3 gives the top views and a half cutted view.

2.1.1. Hot source

The hot source is constituted by a cylinder of heat resistant
steel (30 % Cr) 50 mm in diameter and 220 mm long with a
central hole of 12.7 mm in diameter and 6 longitudinal
grooves regulary spaced around the circunference. The cross
section of the grooves fits with the shape of the extremities
of $FeSi_2$ couples : approximately a semi-circular shape at
the bottom of the grooves with a diameter of 6 mm.

A high temperature electrical resistor in a casing made of
Inconel is placed into the central hole (Reference VULCANIC
type 1008-10 - diameter 12.7 - length 200 mm).

The cylinder with its resistor is fixed on a metallic frame
by 3 screws with the interposition of a disc of ceraminc
fiber.

2.1.2. Cold source

The cold source consists in 3 steel ring with the following
dimensions :

- external diameter 140 mm
- internal diameter 90 mm
- thickness   8 mm
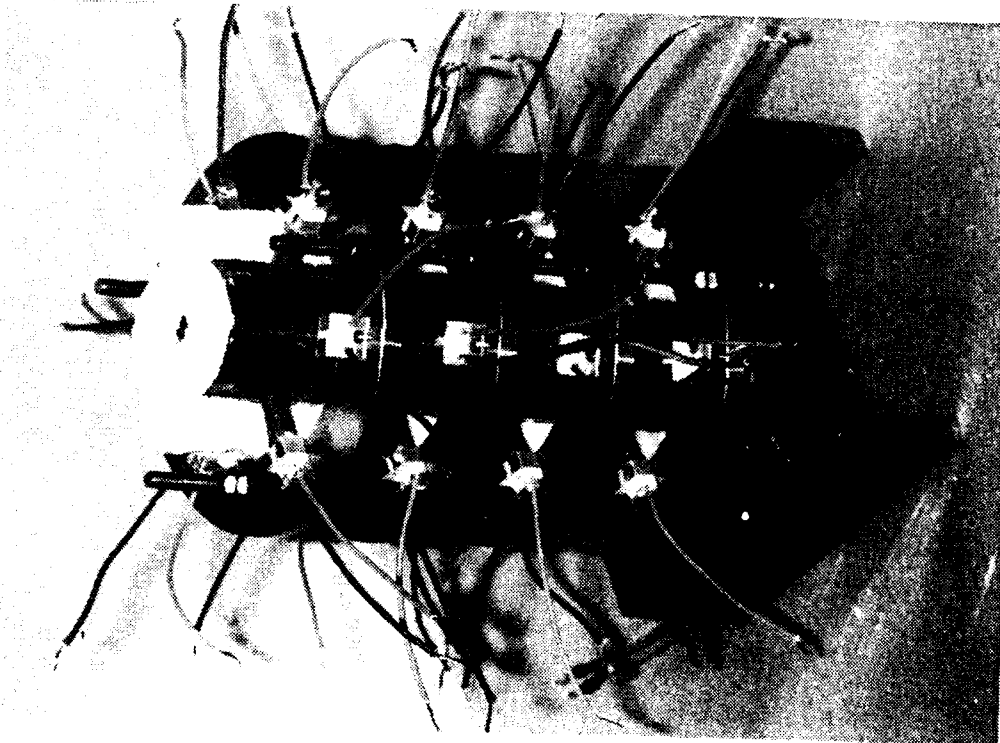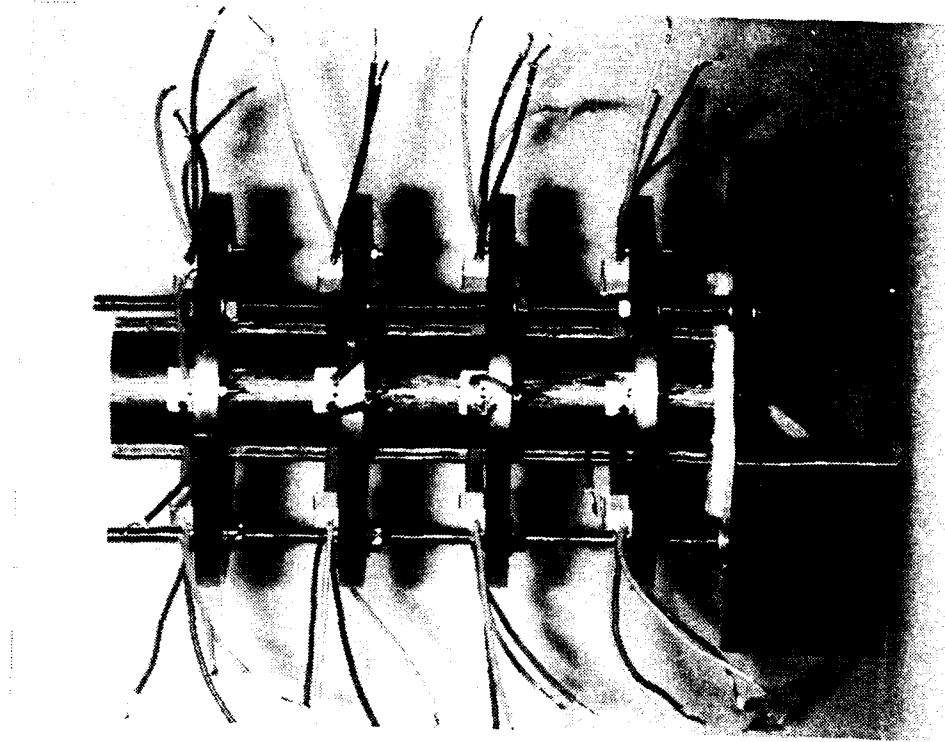
Figures 2.1 and 2.2 : Two views of the experimental arrangement
without its thermal insulation
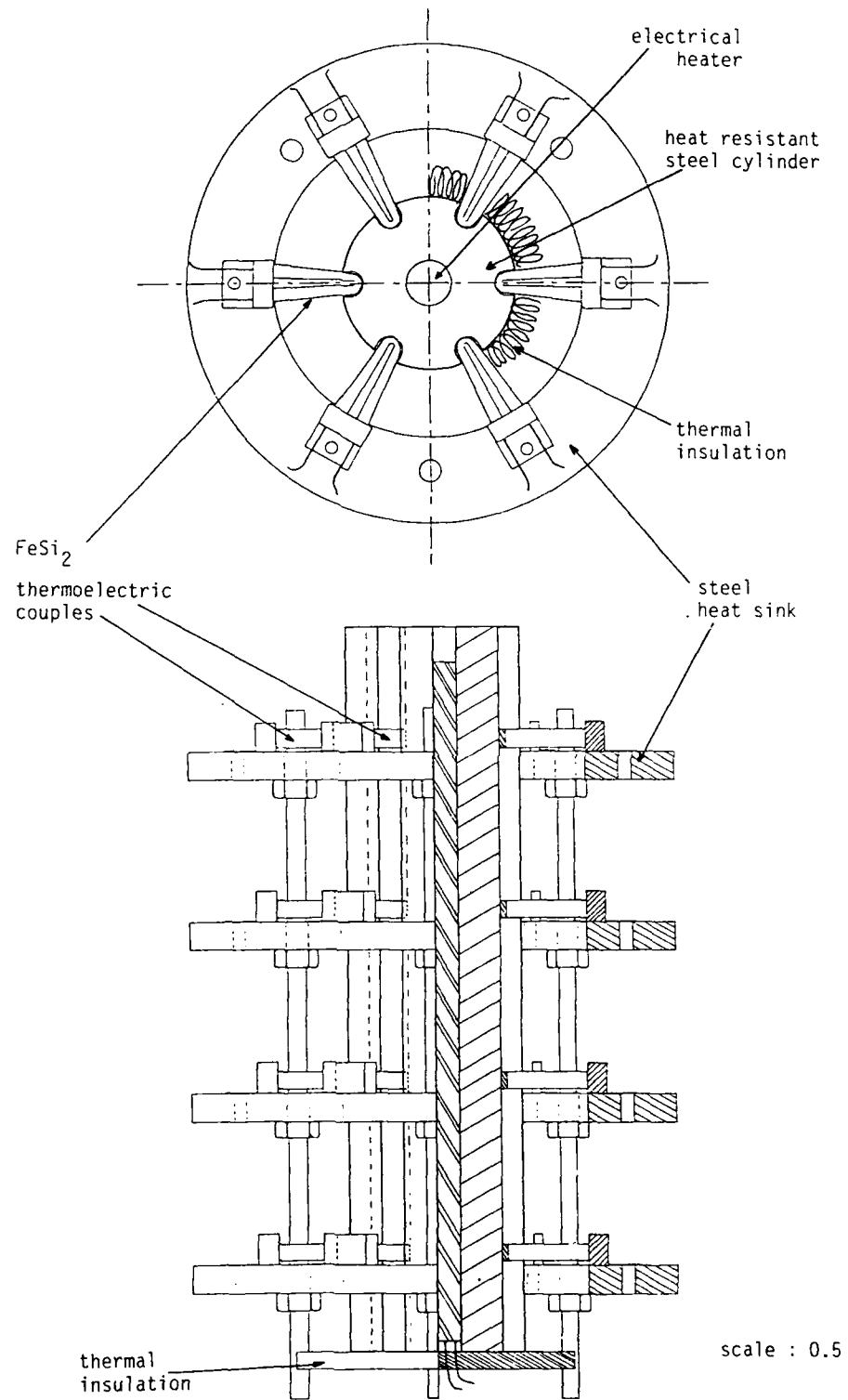
Fig. 2.3- SCHEMATIC OF EXPERIMENTAL ARRANGEMENT

These rings are regularily spaced along the cylindre as shown in the Fig. 2.3. which shows 4 rings. The experience lead us to suppress the fourth ring at the bottom of the cylinder, because it presented a noticeable difference of temperature compared with the 3 others, due to a gradient of temperature existing at the end of the cylinder (> 100°C at 800°C) attached to tho metallic fram.

2.1.3. Thermal insulation and electrical insulation

To minimize the heat losses, the whole external surface of the cylinder is insulated by a layer of ceramic fibers (Kerlane).

The base of the cylinder fixed to the metallic frame is insulated by the interposition of two dises of ceramic fibers each having a thickness of 9 mm. The 3 screws for the fixation are isolated from the epoxy coated stell frame by 2 sheets of mica (~ 1 mm) on each face.

Nevertheless at high temperature the heat losses are noticeable (for a heater temperature of 800°C it is not possible to maintain the hand on the frame). This explains why it was necessary to suppress the steel ring which was the nearest of the base, because the heat losses induce a temperature gradient.

The cylindrical surfaces and the terminal circular surface are insulated by a layer of ceramic fibers (thickness 12 to 15 mm) glued by a refractory cement (Fixwool).

Between the 3 series of thermoelements, the 6 grooves have an insulation consisting of bands of the same ceramic fiber with the appropriate lengths.

For the experiments with no thermoelements the place of their tips is also insulated.

For the experiments with the thermoelements, the space between the two legs of the thermoelements receives a small piece of thermal insulation.

To avoid any electrical shorts between the thermoelements and the metallic cylinder, it is necessary to electrically insulate the tips of the thermoelements.

A first tentative consisted to "paint" the grooves with the refractory cement (Fixwool) used to glue the thermal insulation. The result was negative and this was abandonned.

The electrical insv'ations is obtained by a sheet of mica (thickness ~ 0.3 m placed into the grooves. The inconvenience of this interposition is to reduce the hot junction temperature (and the effective T) and to complicate the temperature measurements (see 3.3).

2.2. Power supply for the hot source

The high temperature electrical resistor (VULCANIC 1008-10) is supplied by the grid (220 V AC, grounded) through an adjustable auto-transformer which allows to obtain the needed value of the electrical power by variation of the input voltage between 0 and 220 V.

The effective power supplied to the resistor is measured using a wattmeter which gives directly the active power.

A voltmeter (KEITHLEY 177) gives the voltage delivered by the auto-transformer.

The Figure 2.4 gives a schematic of the electrical circuit including the external load circuit described below.

2.3. External load circuit

The electrical power generated by the thermoelements is dissipated in an external load circuit.

The circuit comprises :

- a shunt resistor 0.1 V - 3 A for the current intensity
- a voltage measurement for the circuit
- an adjustable load resistance 0-150 ohms.

This load resistance is adjusted at each experiment so as to obtain the maximum power output. The resistance value is measured using an ohmmeter (ESI 1701B).

2.4. Measurements and data logging

The temperature measurements are made using type K thermocouples (Chromel-Alumel) with a metallic sleeving of OD 1.5 mm.

The range of measurement is -100 + 1300 °C.

- 6 thermocouples are inserted into holes of 5 mm deep, drilled in the cylinder as near as possible to the location of the tips of the thermoelements (2 thermocouples for each serie of thermoelements).

- 6 thermocouples measure the temperature of the heat sink (2 thermocouples for each ring).

- 2 thermocouples are placed at the surface of the thermal insulation with a slight pressure.

- 2 movable thermocouples measure the mica surface temperature into the grooves.
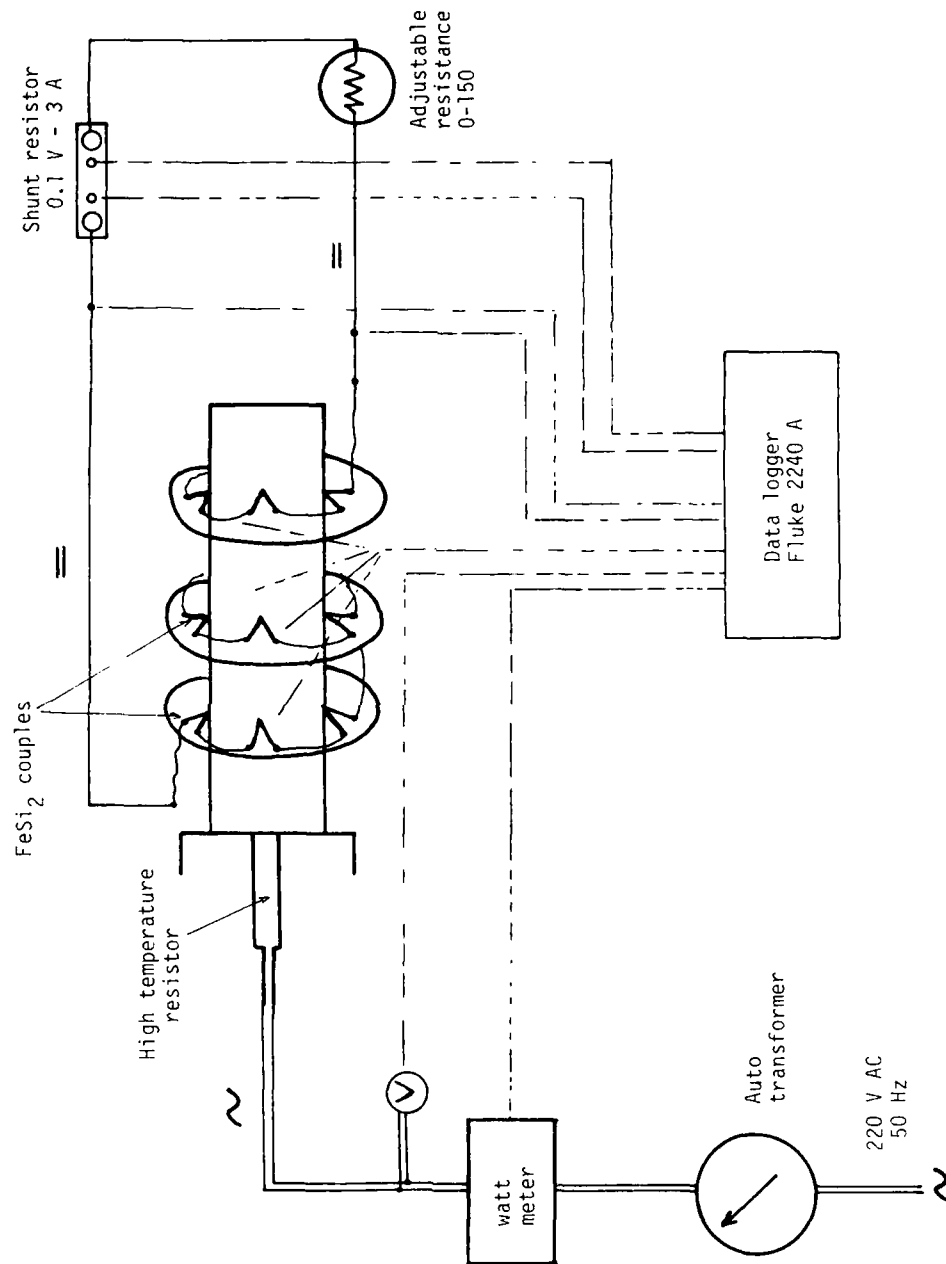
Figure 2.4 SCHEMATIC OF THE ELECTRICAL CIRCUITS

The electrical parameters are measured as following :

- Electrical power for the hot source.
  The effective power measuring device (wattmeter) gives an
  output voltage of 0-10 V corresponding to the range 0-1000 W.

- External load circuit
  . the voltage is measured directly by the data logger
  . the current intensity is measured using a shunt resistor
    0.1 V, 3 A
  . the load resistance is measured independently using an
    ohmmeter ESI 1701 B.

The temperatures and the electrical parameters, except the
measurement of the load resistance, are linked to a data logger
FLUKE, which centralizes all the data.

3 - EXPERIMENTAL CHARACTERIZATION
OF THE FeSi₂ COUPLES

3.1. Experimental procedure

The above described assembly allows an experimental determination of the performances of the FeSi₂ thermoelements.The procedure is the following.

We choose as main parameter the temperature of the heater and we determine experimentally the electrical power to be supplied to the electrical resistance which maintains a given temperature for the heater. Simultaneously the outside surface temperature of the thermal insulation is measured.

The heat losses of the assembly are calculated from these experimental values.

A second set of experiments is made with the 18 (3 x 6) FeSi₂ thermoelements, with their P-N junctions placed into the grooves of the heater and their cold junctions fixed on the rings, which act as a fin for the heat sink. The following values are measured at thermal equilibrium :

- the electrical power needed to maintain a given temperature of the heater
- the ouside surface temperature of the insulation
- the temperature the hot source at the surface of the mica insulation in the grooves.
- heat sink temperature (fin)

The electrical circuit of the thermoelements is then closed on an external load circuit which is constituted by an adjustable resistance. The voltage and the current delivered by the thermoelements are measured and maximum electrical power is determined by adjustement of the load resistance.

This gives an indirect measurement for the internal resistance of the thermoelements because the maximum generated power is reached for an external load resistance equal to the internal resistance.

If the others parameters remain constant, it can be assumed that the difference of the electrical power supplied, at a given temperature of heater, between the determination with the thermoelements and the determination without the thermoelements is equal to the power flowing through the thermoelements.

During the experiments, it was observed that the surface temperature of the insulation was systematically lower for the determination with the thermoelements than the one for the determination without the thermoelements, for a given heater temperature.

3.2. Experimental results

Two sets of experiments are presented, one with no thermoelements, the second with 18 (3x 6) thermoelements. Measurements are done with open circuit and with closed circuit with an external load resistance.

Each measurement is made when the thermal equilibrium is reached within $\pm$ 2°C (in most cases within $\pm$ 1°C). The temperatures are the average values for several thermocouples :

- 6 thermocouples for the heater
- 6 thermocouples for the rings (heat sinks)
- 2 thermocouples for the outside surface of insulation
- 2 thermocouples for the surface of mica in the grooves

The average surface temperature of the mica at the level of a couple is obtained by moving during an experiment the location of 2 thermocouples.

The ambiant temperature varies between 20 and 23°C.

The experimental values are summarized in the tables of the following pages.

Table 3.1 gives the following measurements as a function of the heater temperature :

TS = insulation outside surface temperature
TC = cold source temperature (= fin temperature)
TH = mica surface temperature (=hot junction temperature)
PE = heater electrical power

Table 3.2 shows the variation of the generated electrical power as a function of heater temperature and load resistance.

These values are presented in the form of curves :

- Fig. 3.1 Heating power as a function of the heater temperature for the both case without and with thermoelements
- Fig. 3.2 which gives the different families of temperatures plotted as function of the heater temperature.

The regularity of the curves allows to control the validity of the measurements.

TABLE 3.1

EXPERIMENTAL VALUES : THERMAL MEASUREMENTS

<u>Without thermoelements</u>

Heater temperature ($^\circ$C)	Insulation outside surface temperature T_S ($^\circ$C)	Cold source temperature T_C ($^\circ$C)	Heater electrical power PE (W)
110	–	26.5	19.8
198	55	29.5	40
396	100	38.5	102
598	155	51	190
701	180	58	249
800	210	65	314

<u>With 18 (3 x 6) thermoelements</u>

Heater temperature ($^\circ$C)	Mica surface temperature TH ($^\circ$C)	Insulation outside surface temperature T_S ($^\circ$C)	Cold source temperature T_C	Heater Electrical power PE (W)
111	–	38	34	26.5
198	165	55	43.5	57
396	350	97	64.5	140
599	540	140	85	255
702	630	165	96.5	319
800	720	185	107	400

TABLE 3.2

EXPERIMENTAL VALUES : ELECTRICAL MEASUREMENTS

| Heater temperature °C	Load resistance	Generated		
		voltage V	current mA	power mW
198	26.0	0.457	17.6	8.0
	28.0	0.503	18.3	9.2 *
	32.0	0.505	16.0	8.1
	35.0	0.526	15.0	8.0
	37.0	0.540	14.7	7.9
396	12.0	0.952	80.4	76.5
	14.2	1.050	75	78.7
	18.7	1.205	65.6	79.0 *
	20.9	1.268	61.3	77.7
599	8.3	1.580	193	306
	10.6	1.803	174	313
	12.8	1.986	158	314
	13.8	2.047	154	315 *
	14.4	2.100	149	313
	15.6	2.191	141	310
702	8.3	2.00	246	492
	10.8	2.188	228	499 *
	12.0	2.424	205	497
799	5.5	1.80	377	678
	8.4	2.402	310	746
	9.2	2.577	291	750
	9.8	2.670	281	751 *
	10.5	2.686	279	749
	13.5	3.095	234	725

* maximum power
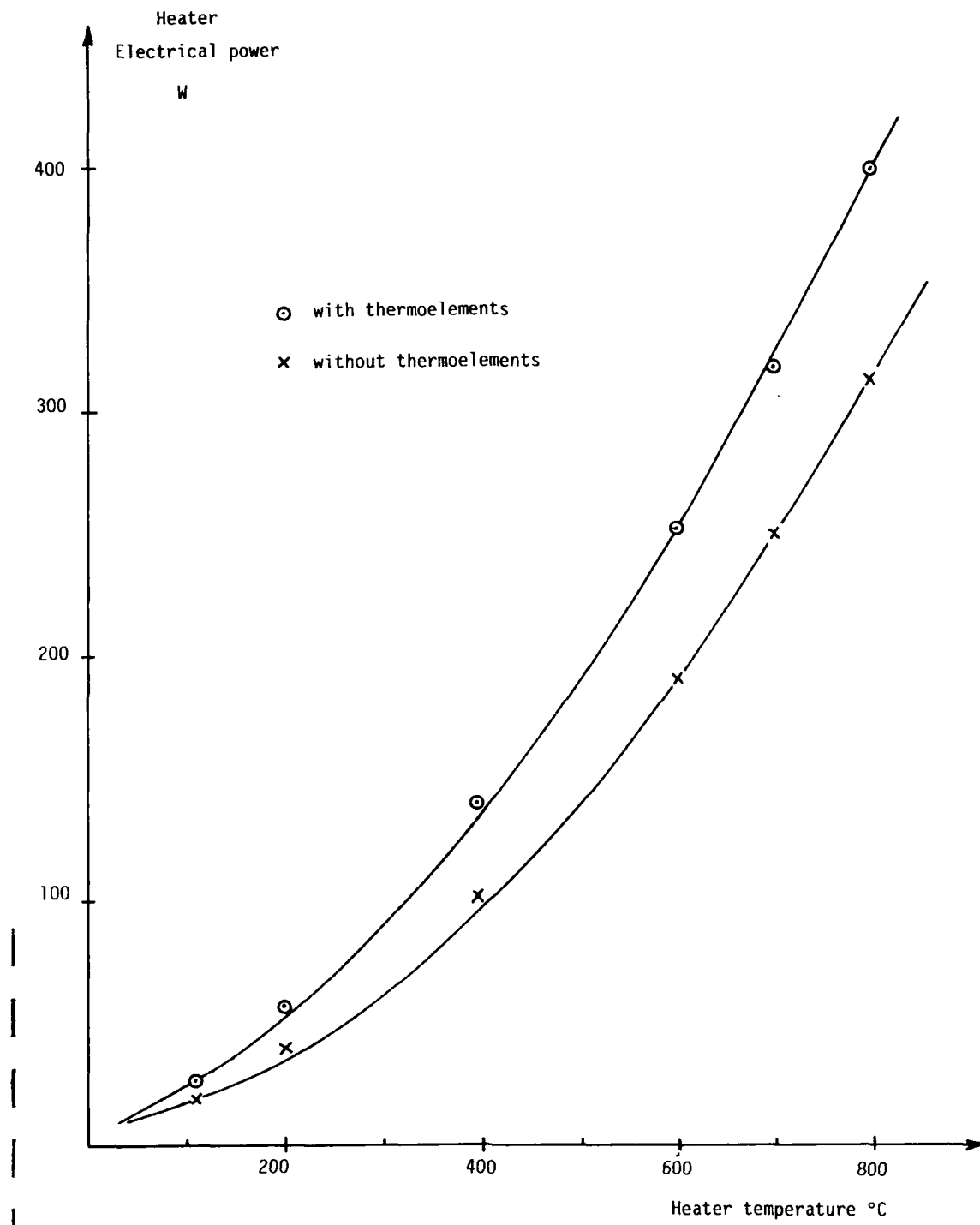
Fig. 3.1
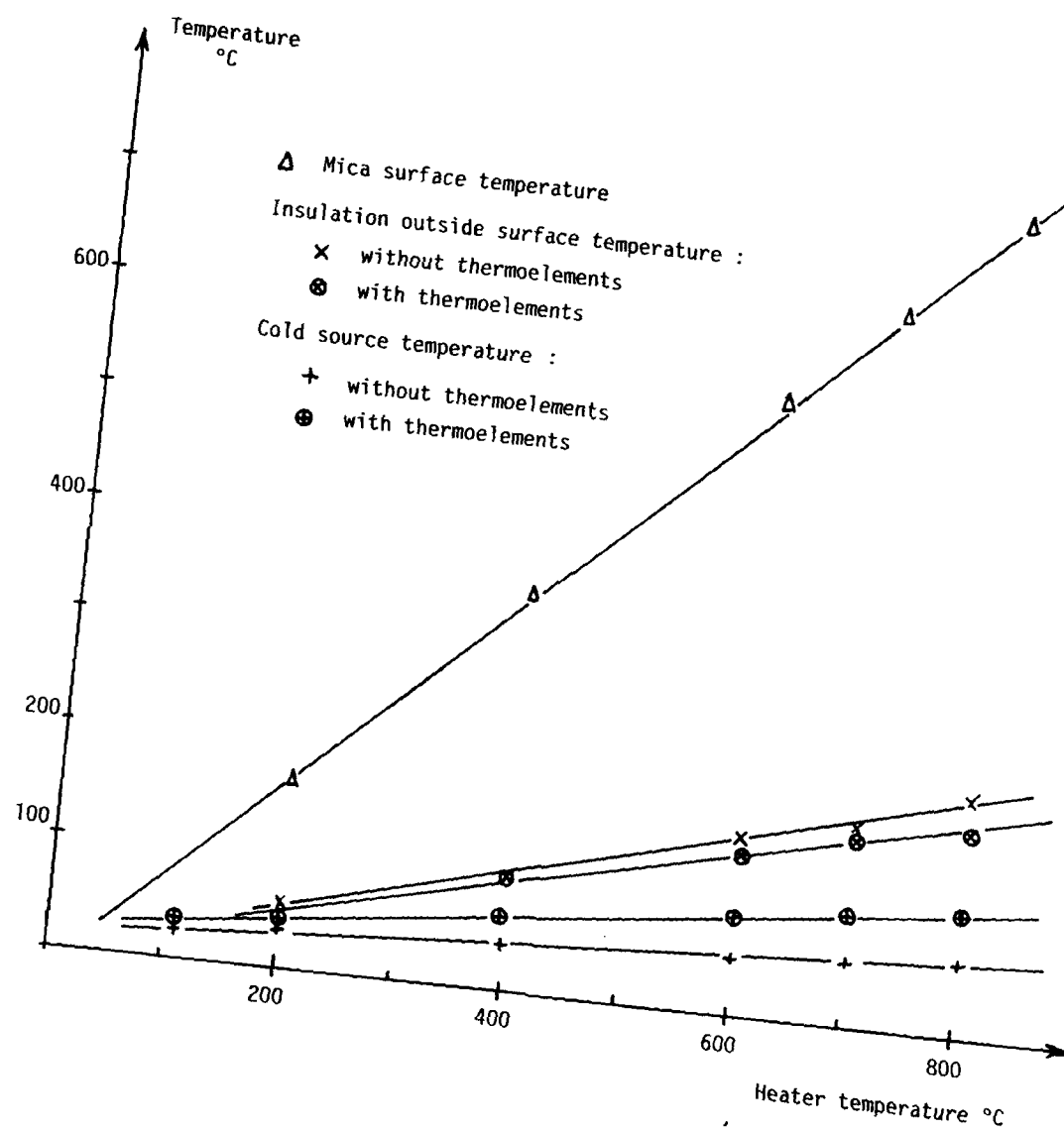
Fig. 3.2

3.3. Experimental difficulties

The main difficulty in this experimental work is to be able to measure the heat flux through the FeSi$_2$ couples, and to measure the hot junction temperature.

The initial prototype was to have a ceramic cylinder around the electrical heater into which the FeSi$_2$ couples were inserted.

It is not easy to machine-tool a ceramic so a ceramic was molded containing the hot junction of one couples. The ceramic shrinkage compelled to abandone this technique.

It was decided to machine-tood a heat resistant steel cylinder with grooves into which the couples would be pressed. Pressure was obtained by the thermal expansion of the core. There was no spring loading at the cold junction.

Initially the couples were cimented into the grooves.

Unfortunately we are not able to master the electrical insulation between the couples and the metallic cylinder. Any electrical contact with the core was a disaster, because the electrical current generated by the couples go through the cylinder.

It was decided to insert in the grooves a thin sheet of mica between the metallic cylinder and each couple.

The problem now is to measure the hot junction temperature of the couples. A direct measurement on the couples had to be abandonned, because the electrical shorts to the measuring parts.

All the thermocouples used were chromel-alumel (type K) with a metallic sleeving. The OD was 1.5. mm. Theoreticaly the junction were electrically insulated of the sleeving but in fact the insulation was not reliable.

It was decided that the best way to obtain the hot junction temperature was to place a thermocouple onto the mica beside the junction.

Au error calculation was made on the accuracy of the "hot junction" temperature measurement.

The error comes from the fact that the FeSi$_2$ couples draws much more heat flux than a thermocouple. The calculation shows that the measurement value can be up to 30°C above the real value.

Another difficult measurement is the outside surface insulation
temperature measurement. The insulating material was compact
(100 kg/m³) the thermocouples were lead on the material under
slight pressure. The real values are probably up to 30°C above
the measurement values, which represents an error in the
temperature difference between the inside and outside
temperature of 5 %.

3.4. Analysis of results

Using the above described procedure, we can reach the thermal
power flowing through the thermoelements.

By adjusting the values of the external load resistance in
closed circuit, the maximum available generated electrical power
is determined, giving simultaneansly the internal electrical
resistance of the thermoelements.

The ratio of generated electrical power to the needed thermal
power is the practical efficiency of the generator.

The values calculated from the experimental measurements are
presented in the following tables, with a comparison with the
expected values obtained from the data of the manufacturer.

On the first table 3.3. one are summarized the calculations
leading to the thermal power and the value of maximum generated
power.

On the second table 3.4. the values of the thermal power
calculated using the values of the manufacturer for the thermal
conductivity are compared with the experimental ones. It gives
also the comparaison between the measured and the expected
values for the electrical resistance.

On the third table 3.5. the values of the measured open-circuit
voltage give the corresponding Seebeck coefficient, which is
compared to the data of Komatsu.

TABLE 3.3

CALCULATIONS ON EXPERIMENTAL VALUES
thermal power and generated electrical power

Heater Temp. °C	Thermal power from heater		PE W	Load resistance Ω	Maximum Generated power (mW)		Effective ΔT (°C) = TH – TC	Efficiency measured %
	with TE W	without TE W			measured	data of Komatsu		
198	57	40	17	28	9.2	16	121	0.054
386	140	102	38	18.7	79	117	285	0.208
599	255	190	65	13.8	316	396	455	0.486
702	319	249	70	10.8	499	558	533	0.713
800	400	314	86	9.8	751	792	613	0.873

TABLE 3.4

CALCULATIONS ON EXPERIMENTAL VALUES
thermal conductance and electrical resistance

Heater temp. °C	Effective ΔT * °C	Average TE temp. * °C	Thermal conductivity K (Komatsu) W/(m.K)	Thermal conductance C for 1 TE $C = 1.391\ 10^{-3}$ K W/K	Thermal conductance C for 18 TE W/K	Thermal power through 18 TE (W)		Internal resistance for 18 TE (Ω)	
						calculated from C	measured	measured	data of Komatsu
198	121	104	11.78	0.0164	0.2949	35.7	17	28	30.2
396	285	207	10.13	0.0141	0.2535	72.2	38	18.7	17.7
599	455	312	9.05	0.0126	0.2265	103.10	65	13.8	13.2
702	533	363	8.61	0.0120	0.2157	115.0	70	10.3	11.4
800	613	414	8.20	0.0114	0.2054	125.9	86	9.8	9.9

* These temperatures are calculated from the mica surface temperature (hot junction) and the cold junction temperature.

TABLE 3.5

OPEN CIRCUIT VOLTAGE MEASUREMENT

Heater temperature °C	Mica surface temperature Hot Junction temperature °C	Cold source temperature °C	Average couple temperature °C	Effective ΔT °C	Open circuit voltage (18 couples) V	Seebeck for 1 couple $\mu V/K$	
						measured	data Komatsu
400.6	353.5	65.2	209	288.3	2.248	433	576
408.0	350.6	61.3	206	289.3	2.325	447	580
624.0	551.7	82.6	317	469.1	3.950	468	558
798.4	730.9	106.9	419	624.0	5.177	461	549

Fig. 3.3

Electrical resistance
for 18 thermoelements

Ohm

+ Experimental values

⊙ Calculated values
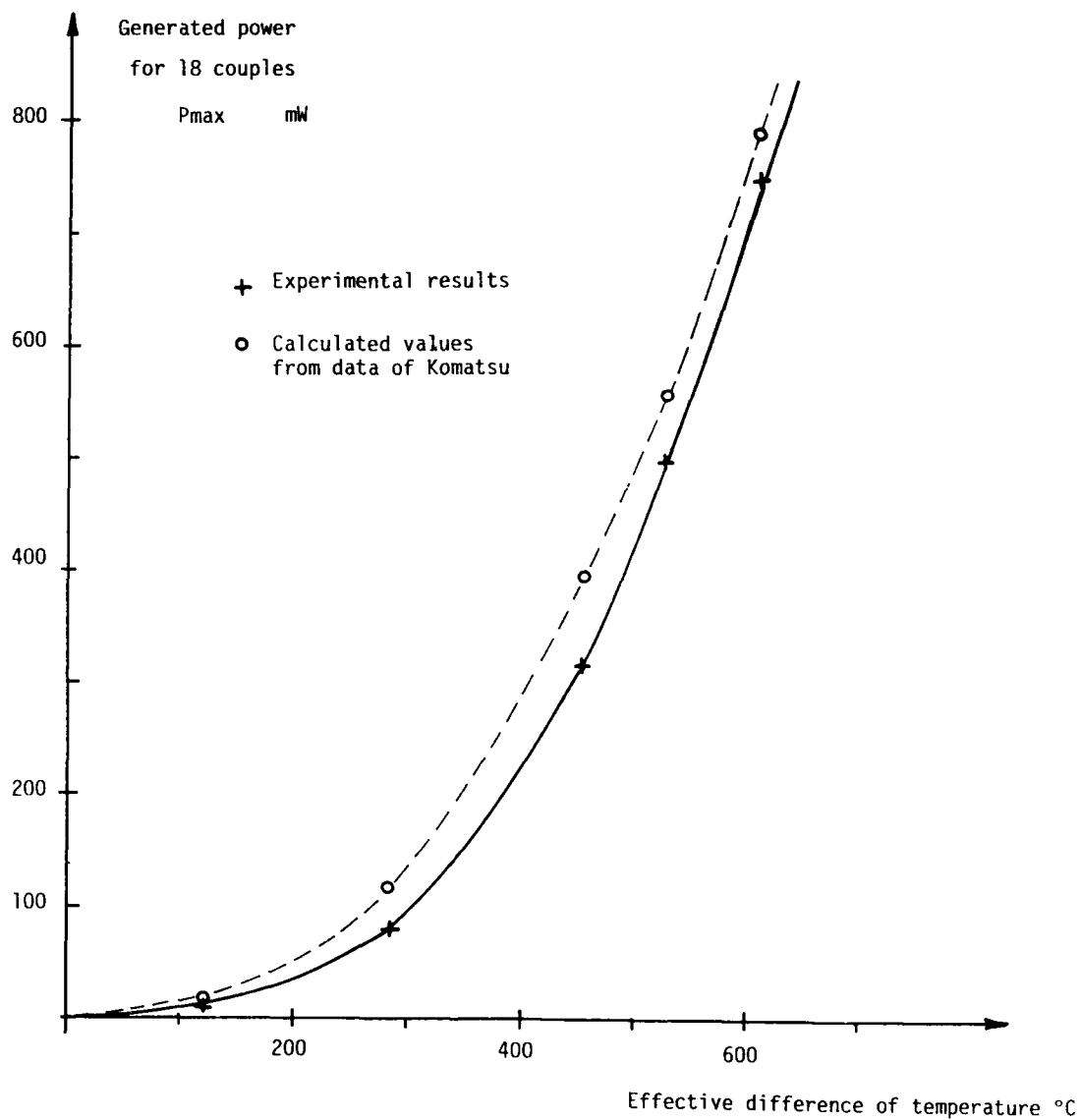from date of Komatsu
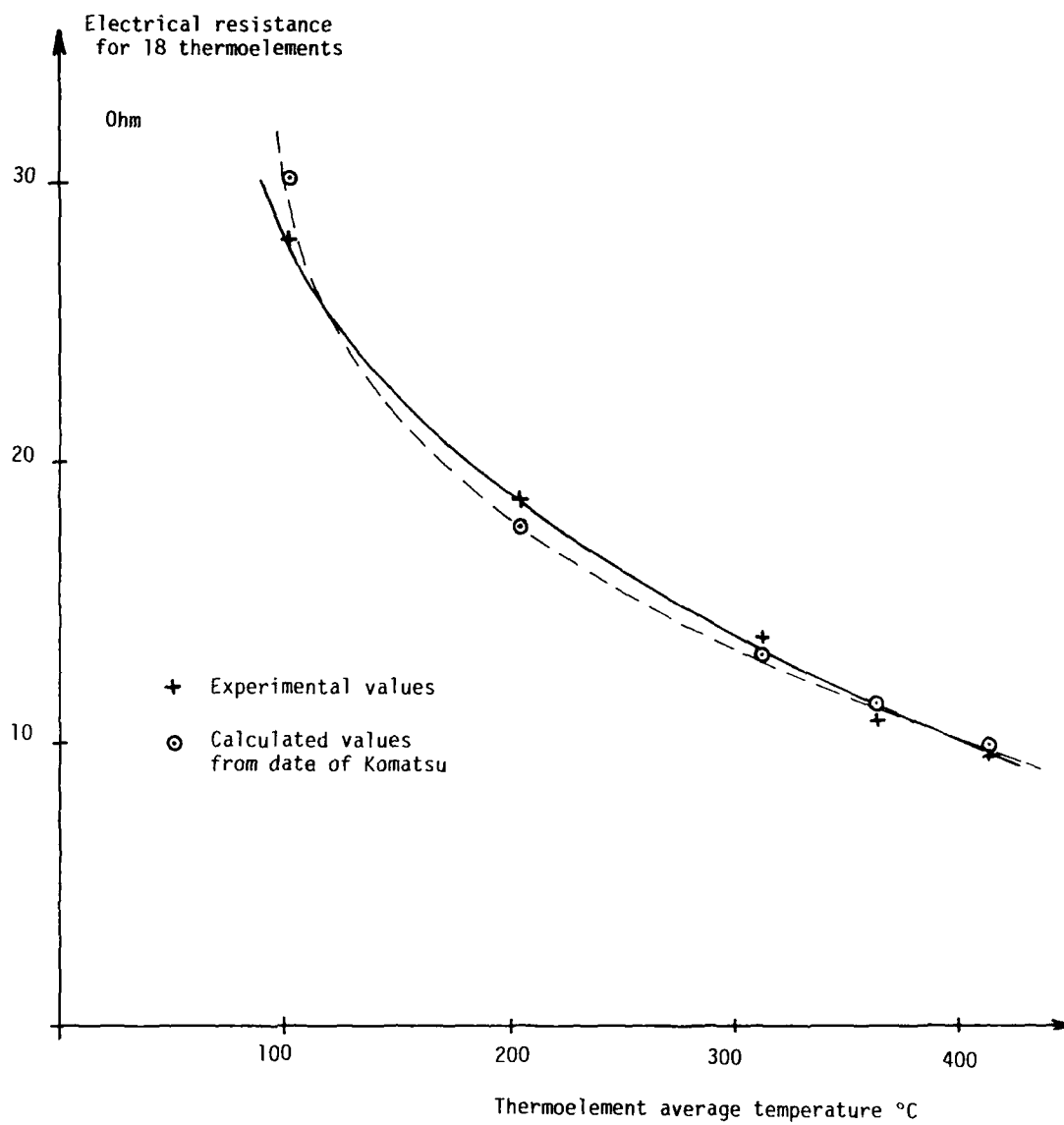
Thermoelement average temperature °C
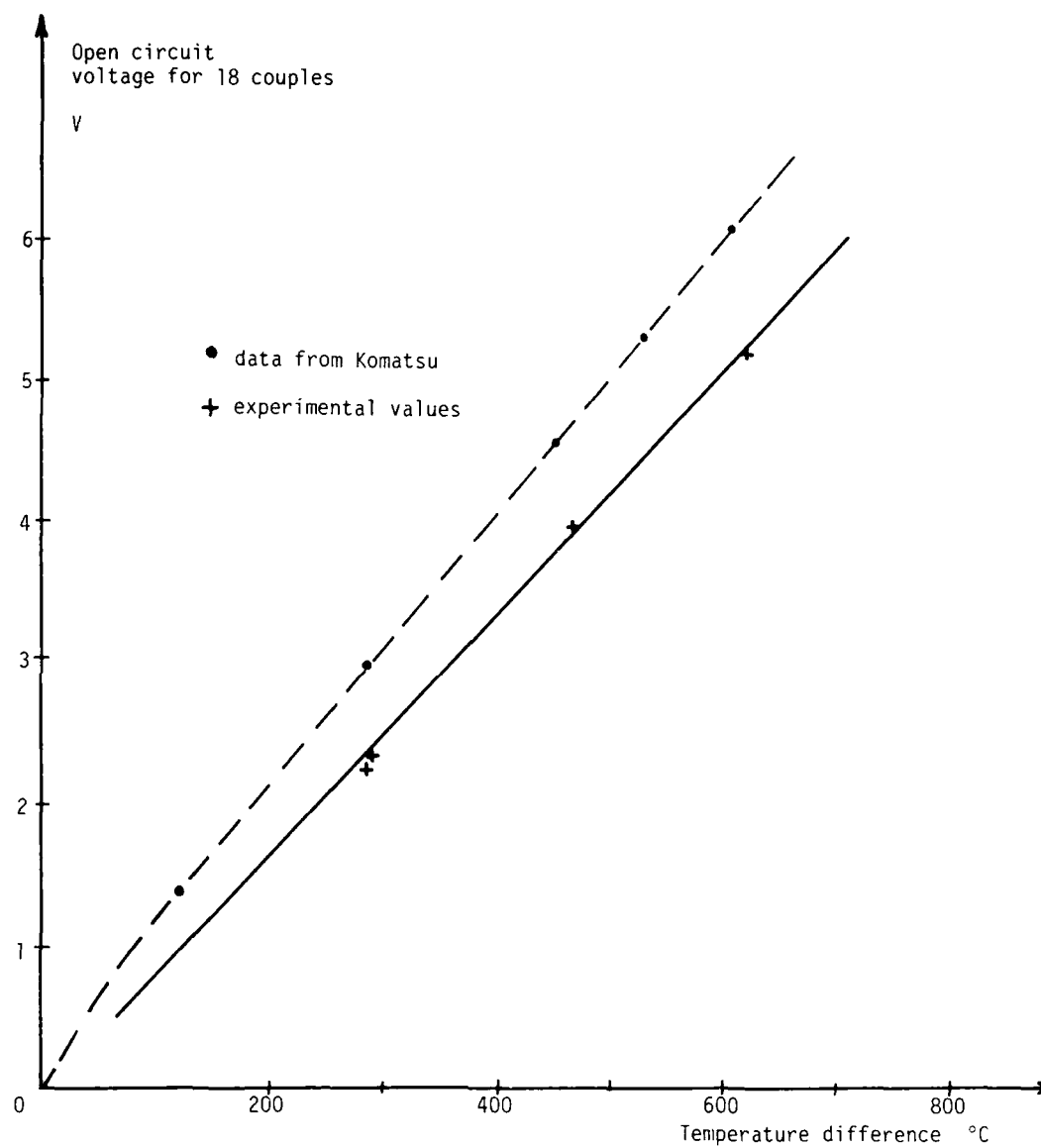
Fig. 3.4

Fig. 3.5

4 – COMPARISON WITH KOMATSU DATA

We present here the comparison betwenn the experimentally determined characteristics and the values taken from the data of Komatsu.

It is often practical to evaluate the quality of a thermoelectric material using the Figure of Merit. This parameter collects the thermoelectronic properties and the electrical properties

$$Z = \frac{\alpha^2}{\rho \cdot k}$$

When one is dealing with a couple, one write :

$$Z = (\frac{\alpha_N + \alpha_P}{R \cdot C})^2$$

These two expressions for Z are analoguous on the condition that the contact resistance at the hot junction is integrated into the material resistance.

For a material :

α = Seebeck coefficient   V/K
ρ = electrical resistivity Ω.m
k = thermal conductivity   W/(m.K)
R = electrical resistance Ω
C = thermal conductance   W/K

with :

$$R = \rho \cdot \frac{\ell}{S}$$

$$C = k \cdot \frac{S}{\ell}$$

ℓ = thickness

S = cross section area

In the case of a couple, if the indices N and P indicate the parameters for each type of material, the following relationships are established :

$$R = \rho_N \cdot \frac{\ell_N}{S_N} + \rho_P \cdot \frac{\ell_P}{S_P} \quad \text{including contact resistance at the hot junction}$$

$$C = k_N \cdot \frac{S_N}{\ell_N} + k_P \cdot \frac{S_P}{\ell_P}$$

If $\ell_N = \ell_P$ and $S_N = S_P$

$$R = (\rho_N + \rho_P) \cdot \frac{\ell}{S}$$

$$C = (k_N + k_P) \cdot \frac{S}{\ell}$$

and the Seebeck coefficient to be used is the sum of the Seebeck coefficients for each type.

$$\alpha = \alpha_N + \alpha_P$$

Thus :

$$Z = \frac{(\alpha_N + \alpha_P)^2}{(\rho_N + \rho_P) \cdot (k_N + k_P)} = \frac{(\alpha_N + \alpha_P)^2}{R \cdot C}$$

It is also possible to use the average values for both types of material = $_N$ + $_P$/2 (indice$_{av}$) where the factor of 4 cancelles out

$$Z = \frac{4}{4} \quad \frac{\alpha_{av}^2}{\rho_{av} \cdot k_{av}}$$

Application to FeSi$_2$ couple

For calculation of the characteristies of the FeSi$_2$ couples we have adopted the following values :

- for electrical parameters

    . length of the electrical circuit

$$\ell_1 = 2 \times 31 \text{ mm}$$

    . cross section area = 17.5 mm²

$$S_1 = \text{cross section of one leg of the couple}$$

So :

$\rho = 2.8226 . 10^{-4} .R \ (\Omega .m)$

- for thermal parameters

    . length $\ell_2 = 25$ mm

    corresponding to the effective length between the hot source and the cold source which are not pinpoints

. cross section area

$$S_2 = 2 \times 17.39 \text{ mm}^2$$

corresponding to the average cross section of the two legs between the mean position of the hot and cold sources.

So :

C = 1.391. 10^{-3} . k (W/K)

The table 4.1 is established as following :

- the Seebeck coefficient comes from the table 3.5
- the electrical resistance from table 3.4
- the thermal conductance from table 3.4, the values related to experimental determination is calculated by :

$$C = \frac{P}{\Delta T} = \frac{\text{measured thermal power}}{\text{effective } \Delta T}$$

The calculated Figure of Merit from experimental values is very close to the one calculated from data of Komatsu, despite the fact that we found some difference for the Seebeck coefficient and the thermal conductance.

The lower value for the Seebeck coefficient is compensated by a lower value for the thermal conductance.

It is noticeable to remark that the experimental values of generated power are in good agreement with the predicted ones (see table 3.3. and Figure 3.3) which confirm that the Figure of Merit is a good parameter to evaluate and compare the efficiencies.

It is striking that the Seebeck coefficient from the Komatsu data decreases by 10 % from 100 to 400°C while our data indicates that the Seebeck increase by 5 % for the same average temperature range.

The thermal conductances values are different. We found a constant between 100 and 400°C average temperature. The Komatsu values decrease by 30 % over the same temperature range. At 400°C the Komatsu value is 50 % greater than our value.

The only explanation is that the Komatsu data is from measurements with small ΔT's and our measurement is with large ΔT's and we see the Komatsu data that the Seebeck and the thermal conduction are not linear as a function of temperature.

TABLE 4.1

COMPARISON BETWEEN MEASURED VALUES AND CALCULATED VALUES FROM DATA OF KOMATSU

Heater Temp. °C	Effective ΔT (°C) $T_H - T_C$	Average Temp. T_{av} (°C)	Seebeck (µV/K)		Resistance (Ω)		Conductance (W/K)		$Z \times 10^4$ (K^{-1})	
			measured	Komatsu	measured	Komatsu	measured	Komatsu	measured	Komatsu
198	121	104	441	614	1.556	1.678	0.0078	0.0164	0.16	0.14
396	285	207	448	576	1.039	0.983	0.0074	0.0141	0.26	0.24
599	455	312	464	559	0.767	0.733	0.0079	0.0126	0.36	0.34
702	533 .	363	465	553	0.600	0.633	0.0073	0.0120	0.49	0.40
800	613	414	466	549	0.544	0.550	0.0078	0.0114	0.51	0.48

The 3 values Seebeck, electrical resistance and thermal conductance are those for one couple.

5 – COMPARISON WITH LABORATORY MATERIAL

(UNIVERSITY OF KARLSRUHE)

Professor Ulrich BIRKHOLZ of the University of Karlsruhe (Federal Republic of Germany) recently presented papers on Iron Disilicide (Cardiff 1987 and Arlington 1988).

These papers indicate that for a couple with a total cross section (N + P) of 188 mm² and a lengh of 12 mm, $\Delta T = 600$ K generates around 1 W with the cold junction at 220°C.

The Komatsu material operating under the same conditions gives per couple 43 mW. The cross section of the KOMATSU couple is 35 mm², the effective lenght of the couple is 31 mm.

The difference between the two materials from KOMATSU and from the University of Karlsruhe is so great that we have analysed the two papers that Birkholz has co-authored.

5.1. Material characteristics

To calculate the properties we have used the dimensions of the couples given in the paper presented at Arlington Texas 1988 "Conversion of waste exhaust heat in automobiles using FeSi$_2$ thermoelements".

The dimensions we have used are the following.

Ø 15.5

12.1

3

9.1

0.1
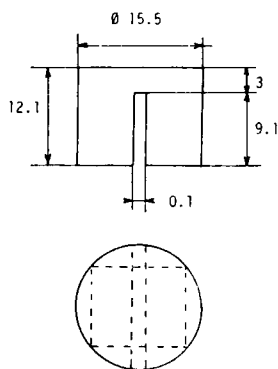
The total contact area at hot junction it : S = 188.7 mm² (circular disc).
The cross section of the each leg is : 93.5 mm²

The length of each leg is equal to 9.1 mm.
We have estimated the resistance of the disc that joints the two legs together at the top. We have taken this resistance is equal to that of a rectangular block of cross section 12 x 3 mm and a length of 7.8 mm.

This gives for the top connecting part :

$$R = \rho \ \frac{\ell}{S} = \frac{7.8.10^{-3}}{3.12.10^{-6}} \quad (\Omega)$$

The total resistance of the couple becomes :

$$R = \rho \cdot \left(\frac{2 \times 9.1 \cdot 10^{-3}}{93.5 \cdot 10^{-6}} + \frac{7.8 \cdot 10^{-3}}{3 \times 12 \cdot 10^{-6}}\right) = \rho \cdot 0.414 \cdot 10^3 \ \Omega$$

or : $\rho = R \cdot 2.431 \cdot 10^{-3} \ \Omega \cdot m$

The text presented in Cardiff 1987 :
"Semiconducting FeSi$_2$ thermocouples for power generation" gives
Fig. 6 the resistance of a couple as a function of the temperature
difference see Fig. 5.1

Using the above relation ship between R and the following table
is obtained. The paper gives two curves represented by ● and O
corresponding to two different materials.

ΔT	Tav	R mΩ		ρ $\mu\Omega \cdot m$	
K	°C	●	O	●	O
0		60.9	37.4	148.0	90.9
200	187	30.2	25.9	73.4	63.0
400	337	25.9	24.2	63.0	58.8
600	512	21.6	20.7	52.5	50.3

In a similar way we have calentated the Seebeck coefficient using
Fig. 5 of the Cardiff paper that gives the open voltage as a
function of temperature difference (See Fig. 5.2) and the Fig. 7
of the same paper (See Fig. 5.3) to obtain the maximum power
output.

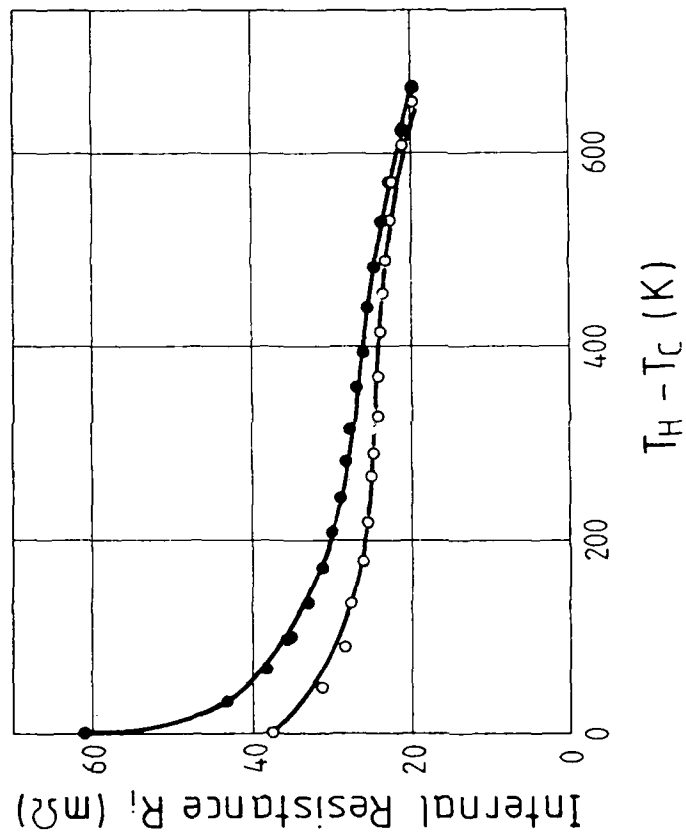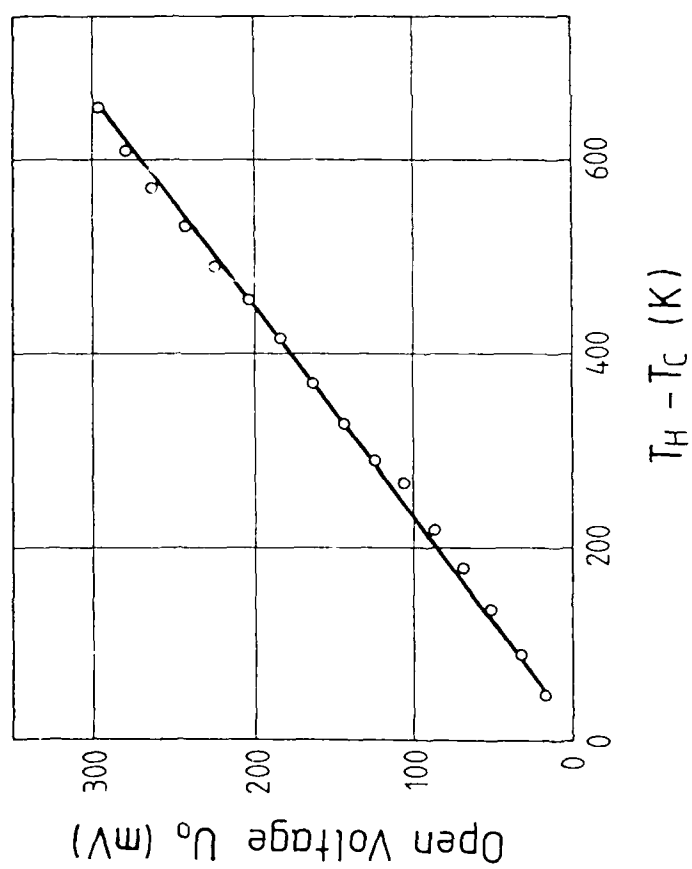| ΔT	ΔV	α	Pmax	Tcold		Thot		Tav
K	mv	μV/K	mW	K	°C	K	°C	
200	83	414	70	360	87	560	287	187
400	177	442	325	410	137	810	537	337
600	268	447	900	485	212	1085	812	512

Figure 5.1

Figure 5.2
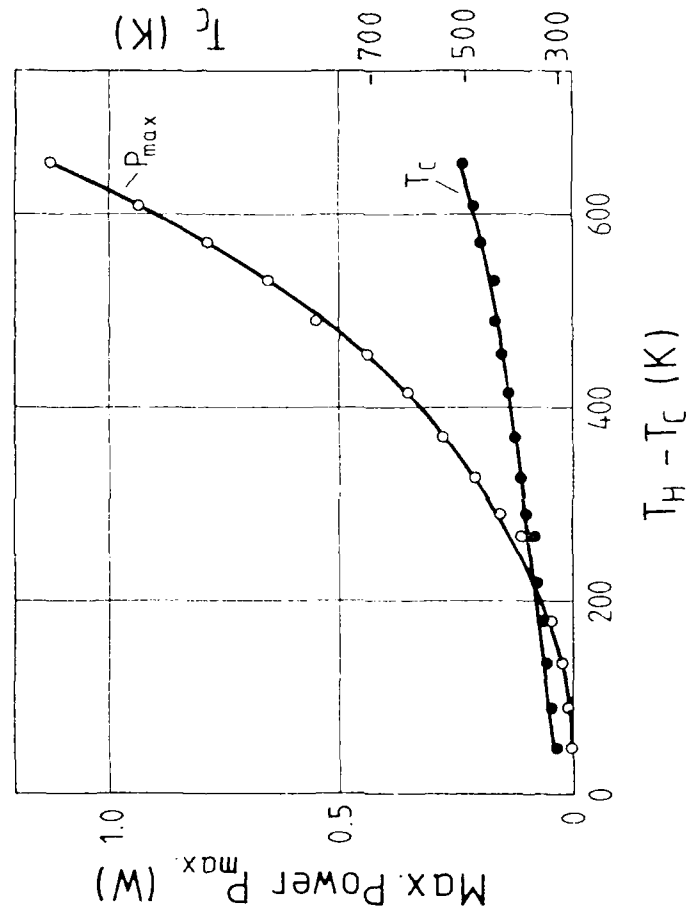
Figure 5.3

The paper presented at Arlington announces a thermal conductivity of K = 5 W (m.K). This values is from a bibliography (Waldecker et al, 1973).

Using these values one can calculate Z the figure of Merit

For $\Delta T = $ 400 K (Tav = 337°C) for the average material $\frac{N+P}{2}$

$$ Z = \frac{(442 \ 10^{-6}/2)^2}{63 \ . \ 10^{-6} \ x \ 5} = 1.55 \ . \ 10^{-4} \quad K^{-1} $$

This value is to be compared to the value for the Komatsu material for Tav = 330°C (ΔT = 600 K)

$$ Z = 0.43 \ . \ 10^{-4} \quad K^{-1} $$

The difference can come of the difference of the quality of the material $FeSi_2$, nevertherless there is an uncertainty in value of the thermal conductivity.

5.2. Power output

The cross section of the Komatsu couple is

$$ S = 2 \ x \ 17.5 = 35 \ mm^2 $$

The University of Karlsruhe couple gives :

$$ S = 2 \ x \ 93.5 = 187 \ mm^2 $$

The ratio of the two cross section is 5.3.

The length ℓ of one leg is :

– for Komatsu : 31 mm
– for University of Karlsruhe : 12 mm

The power output is proportional to the ratio S/ℓ .

For the Komatsu couple   : S/ℓ = 1.13 mm
    the Karlsruhe couple : S/ℓ = 15.6 mm

Our experimental set.up has 18 Komatsu couples

so : S/ℓ = 18 x 1.13 = 20.3 mm

With a temperature difference between the hot and cold junctions of 613 K we generate 0.75 W with the 18 Komatsu couples.

For the same temperature difference $\Delta T = 600$ K one large couple of the University of Karlsruhe gives 0.9 W.

For the same value of S/ℓ , if the Komatsu material has the same properties as the Karlsruhe material, it should give a power output of :

$$P_E = 0.9 \ . \ \frac{20.3}{15.6} = 1.17 \ W$$

Our measurement would give 0.75 W which is 64 % of what Karlsruhe material gives.

The University of Karlsruhe material gives about 50 % more electrical power than the Komatsu material.

This statement is based on experimental results.

Concerning the efficiency (ratio of electrical power to the thermal power going through the couple) we have valid measurements for the Komatsu material. For the other material the announced efficiency is based on a value of the thermal conductivity we have not measured.

A real comparison can only be made after a single couple has been the object of experimental measurements analoguous to the ones made with 18 Komatsu couples on a heat flux prototype.

5.3. POTENTIAL APPLICATION

The University of Karlsruhe developed with Porsche AG an
application for the conversion of waste heat in automobiles.

A typical couple mounting is shown in Fig. 11 of the Arlington
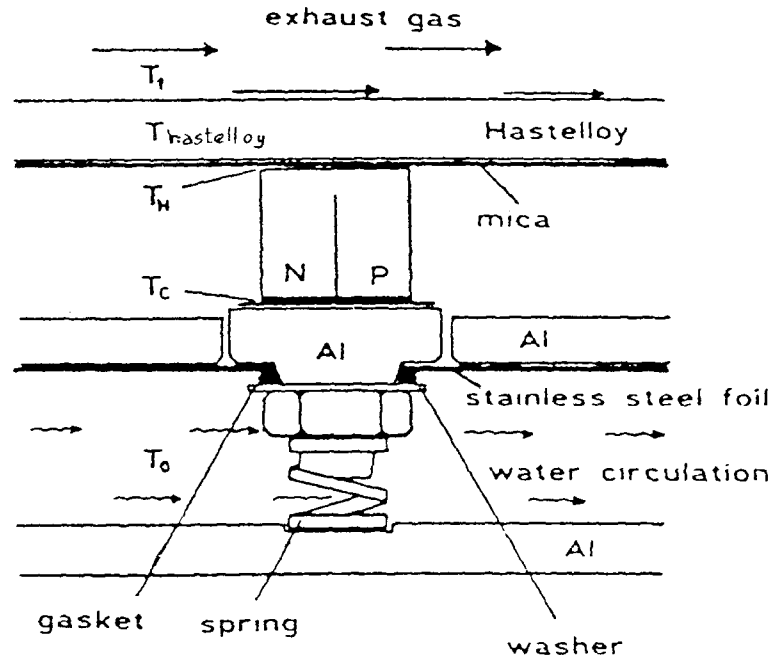paper. It is given below in Fig. 5.4.

Fig.11 Strain relief construction using a
stainless steel foil

Figure 5.4 COUPLE MOUNTING

This technology is very well suited for powers of 10 W or more.

The efficiency seems to be of around 3 %. We explain this higher
value by the fact that the hot junction temperature is well
localised at the end of the couple, while a flame involves a
volume at the hot end.

6 — FLAME PROTOTYPE

Our experimental data for electrical power confirms within a few percent the Komatsu data. We can therefore use the graph of Fig. 1.4 which gives the electrical power versus the temperature difference between the hot and cold junctions.

The maximum operating continuous temperature of the hot junction is 800°C, with a maximum temperature for discontinuous operation of 830°C.

The pratical maximum temperature difference is between 700 and 750°C which leads to a power output for a couple of around 65 mW.

Under load the voltage per couple is around 200 mV.

To generate 5 W about 75 couples are necessary.

A prototype must be optimized from the thermal point of view, so as to obtain the maximum ΔT on the FeSi$_2$ couples.

It is first necessary to dimension the gas duct.

The couples should be on a radius of around 40 mm.

It would be advantageous to have a central core with a radius of 30 mm. On the circumference one can place 16 couples.

Five series are required with an axial pitch of 25 mm giving a length of 125 mm; the overall dimension with a simple gas burner with no moving parts would be 200 mm diameter and a length of 200 mm. See schematic Fig. 6.1 page 86.

Another design would be based on a flat plate that could be placed above a fire.

To place 80 couples with a spacing between couples of 10 mm, the overall dimensions of the flat plate are 200 x 200 mm with a height of 80 mm. See schematic Fig. 6.2 page 87.

The Komatsu couples are adapted for small powers of the order of 1 W. For powers above 1 W many couples are necessary.

A typical application which is used industrially is presented in a small article of Science and Technology in Japan (March 1988).

A new couple is announced can be operated at a slightly higher temperature (850°C) in Techno Japan (Vol. 20 August 1987).
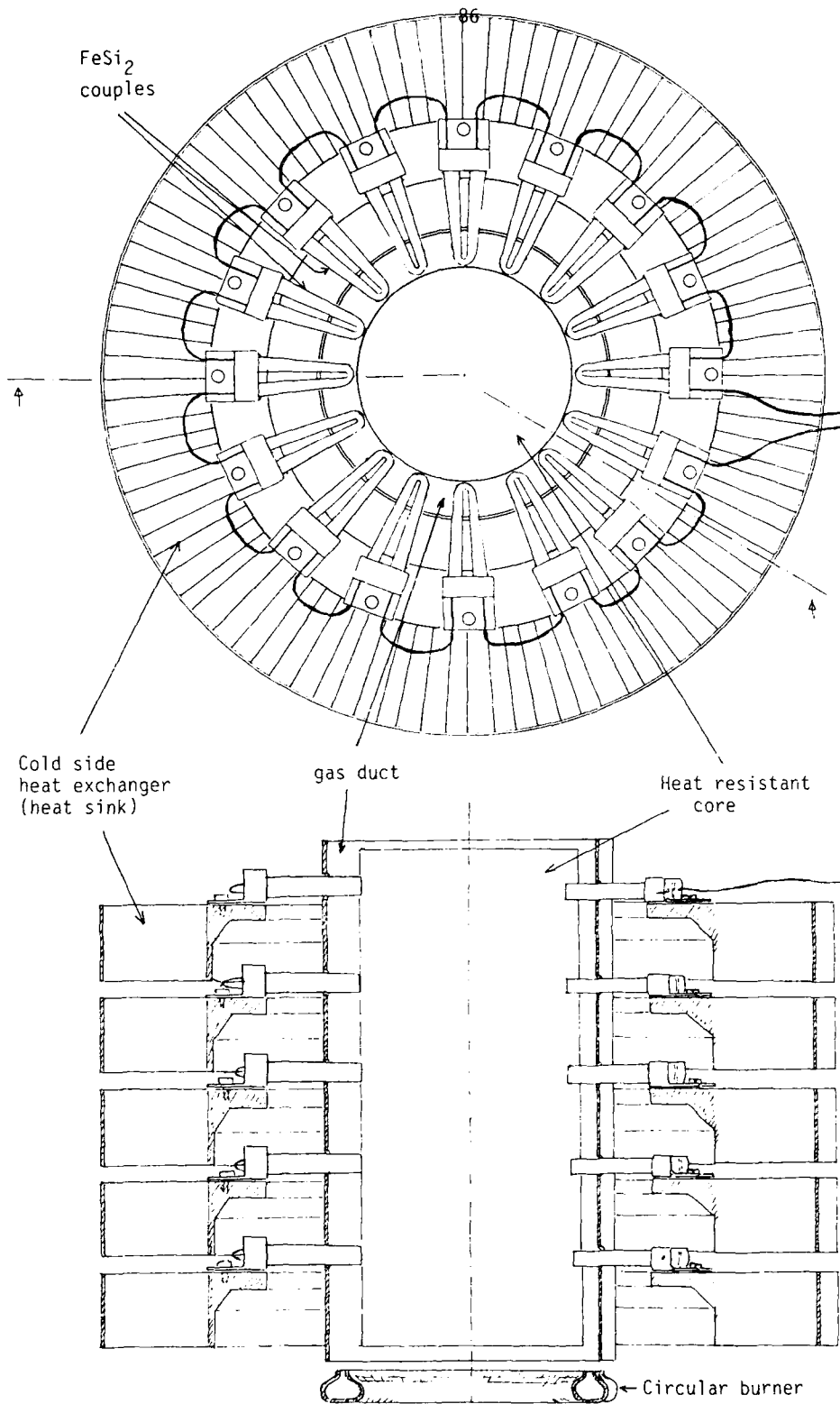
FeSi$_2$
couples

Cold side
heat exchanger
(heat sink)

gas duct

Heat resistant
core

←— Circular burner

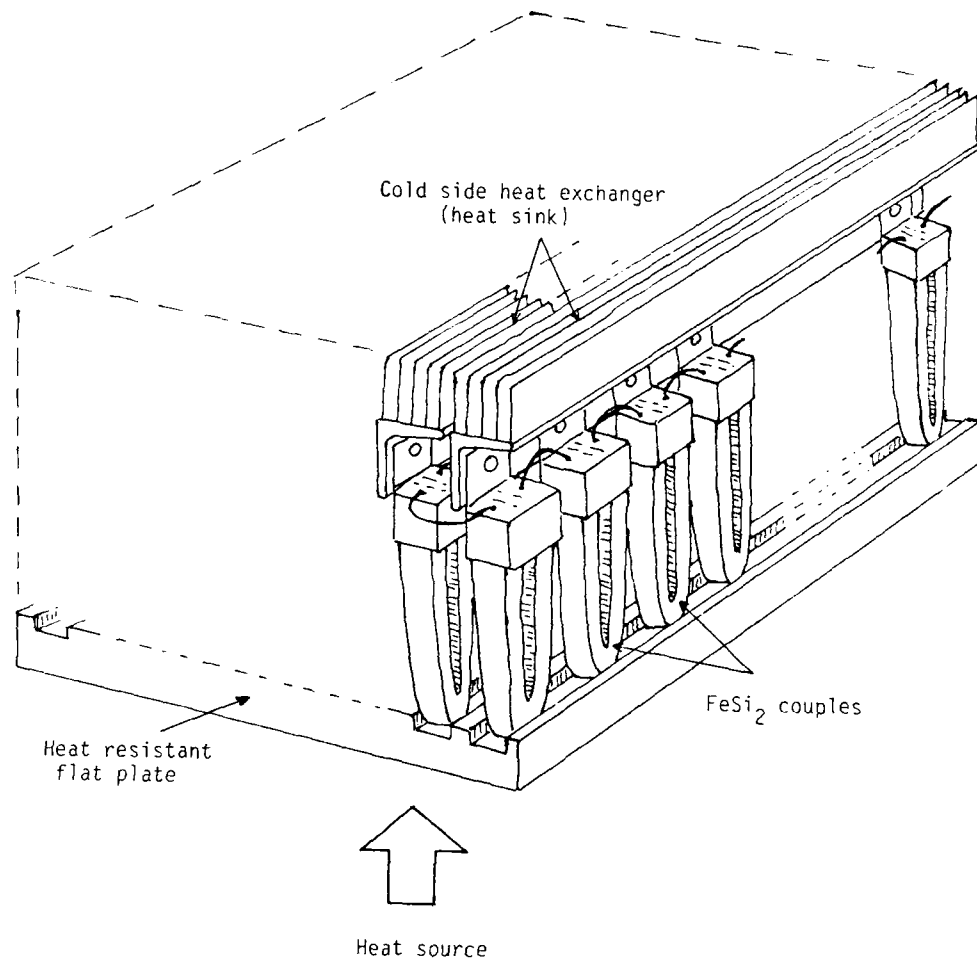FIGURE 6.1 FLAME PROTOTYPE WITH GAS BURNER

Figure 6.2 - FLAT PLATE TEG

DIVERS

Thermoelectric Conversion Element to Be Merchandised

A pair of two dissimilar metal wires joined together as one, is well known by the name 'metallic thermocouple', and is widely used in temperature measurement devices for various machines, instruments and tools.

A different type of thermocouple, a combination set of p-type and n-type semiconductors, is utilized for obtaining electric power from heat by direct conversion. This type of couple is called a thermoelectric conversion element (TCE) or a semiconducting thermocouple as distinguished from metallic thermocouples. Suitable materials for TCE are semiconducting compounds and alloys with metallic conductivity properties. Certain types of TCE's, such as Bi-Te and Pb-Te system compounds and Si-Ge system alloys, are already in practical use as *electric power sources in such places as* distant isolated regions, on the sea bottom and in space.

A TCE recently developed and merchandised by Komatsu Electronics, under the technical guidance of the National Research Institute for Metals, is a sintered iron disilicide with the following properties:

(1) It features a large thermoelectric power force, and the voltage between the two ends of the TCE is measured at about 0.5 V when the temperature difference between the TCE's junction and both branches are at 800 K.

(2) High performance TCEs are available in spite of low production costs and an extremely simple manufacturing process which uses composite materials made from low purity industrial utility grade materials (purity 98%).

(3) The heat and oxidation resistances are high. These TCE's are capable of maintaining their stability in heats of 1200 K or higher.

(4) The thermal shock-resistancy is high. No appreciable performance deterioration was detected after a 100.000 series repeat test of adding heat by gas flame and cooling it in cycles.
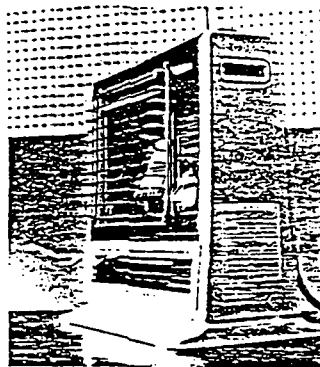
Photo shows a simple thermoelectric generator designed as a visual aid to demonstrate the continuous rotations of a small fan driven by the power of a small TCE weighing only 0.9 g with an alchol lamp acting as the heat source. Other applications for TCE's include instantaneous ignition devices for gas appliances (ranges, ovens, heaters) and automatic temperature control gas boilers.

Fig. shows a gas heater applying a thermomodule made up of a number of TCE's. The heater is devised to blow out hot air at 333K to the front of the heater by a blower which is driven by electricity generated by the TCE's arranged around the gas burner. In other application examples, TCE devices have been used to supplement power for functioning electronic circuits built in gas and kerosene apparatuses. ☐
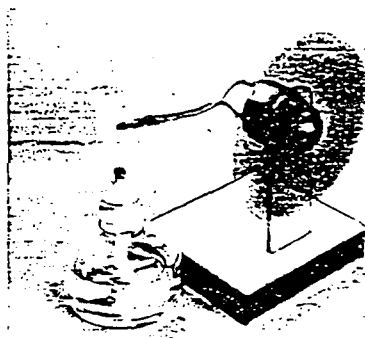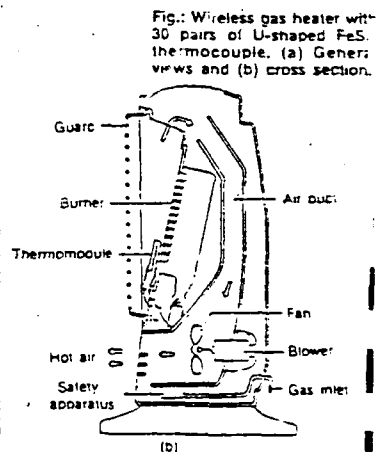

An extremely simple thermoelectric generator.

Fig.: Wireless gas heater with 30 pairs of U-shaped FeS. thermocouple. (a) General views and (b) cross section.

Labels: Guard, Burner, Thermomodule, Hot air, Safety apparatus, Air duct, Fan, Blower, Gas inlet

(a)　　(b)

March 1988

Multilayer Thermoionic Element Developed

The National Research Institute for Metals, together with Komatsu Electronics Co., Ltd., has developed a new type of electric power generating element. It use the principle that when the edge of an element is heated at 850°C, an electric voltage of 0.5V is generated. This element is composed of p- and n- semiconductors. The p-semiconductor is of FeSi added with manganese and the n-semiconductor is of FeSi added with cobalt.
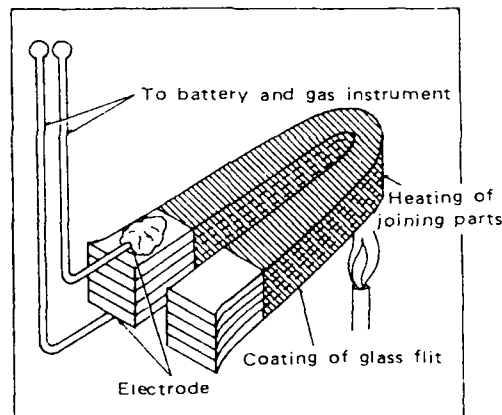

Fig. 1. Multilayer thermoionic generator element

7 – CONCLUSIONS OF SECOND PART

A small thermal flux prototype was built, the maximum electrical output is 0.75 W with 18 couples.

The material properties announced by the manufacturer of the couples Komatsu were checked. We find the thermal conductance given by Komatsu is 50 % greater than what we found. We find also up to a 20 % lower Seebeck coefficient, but we find a Figure of Merit a few percent higher.

The measured electrical powers we find, are 5 % below those predicted by Komatsu. Considering the experimental errors involved, we can consider the Komatsu values are valid.

The measured thermal power flowing through the couples was found to be 30 % below the values calculated from Komatsu data.

The small prototype required 86 W going through the couple to generate 0.75 W. The efficiency of the couples alone is 0.87 %. The prototype unfortunately could not be operated with the hot junction of the couples at 800°C. The maximum reached was 720°C.

The heat losses from the unit represented 314 Watts. The overall efficiency of a flame generator depends enormously of the design. A flame unit will have an efficiency below 0.2 %

We have also summarly examined the use of the couples against a hot side heat exchanger instead of in a flame.

This set up is better suited for generators of more than 10 W.

Nevertheless a power of 10 W is the range where both set-ups : hot junction in a flame and hot junction against a heat exchanger are valid.

GENERAL CONCLUSIONS

Iron disilicide is doped with cobalt to obtain the N type material. The P type is obtained either by Manganese (used by komatsu commercially) or by Aluminium.

The Manganese gives a Z of around $0.5 * 10^{-4}$ K^{-1} while the Aluminium is supposed to give $Z = 2.0 * 10^{-4}$ K^{-1}.

An amorphous material which can only be produced as a thin film appears to have much better properties. This geometry is not applicable for the technology object of this study.

From the experimental point of view we have found that the performances announced by the manufacturer are correct.

The efficiency of the Komatsu couple is of 0.8 % with a temperature difference of 600'C. The maximum efficiency of the couple alone without the outside heat losses is approximately of 1 %.

The overall efficiency with a heat source such as a burner could be expected to be around 0.2 %.

The "flame technology" is definitely the best and the simplest for powers around 1 W.

When 10 W are required, the flame technology requires around 150 couples. In this range large couples with their hot junctions attached to a heat exchanger appear to have an efficiency of the couples alone to be around 3 %. A unit built in this manner would probably be more compact but more costly.

Improvements in the characteristics of this material are probable.

It is possible that the couple efficiencies may reach 3 to 5 percent.